

Estimating surface soil moisture from SMAP observations using a Neural Network technique

J. Kolassa^{a,b,*}, R.H. Reichle^b, Q. Liu^{c,b}, S.H. Alemohammad^d, P. Gentine^d, K. Aida^e, J. Asanuma^e, S. Bircher^l, T. Caldwell^m, A. Colliander^f, M. Cosh^g, C. Holifield Collinsⁿ, T.J. Jackson^g, J. Martínez-Fernández^h, H. McNairnⁱ, A. Pachecoⁱ, M. Thibeault^j, J.P. Walker^k

^a*Universities Space Research Association/NPP, Columbia, MD, USA*

^b*Global Modelling and Assimilation Office, NASA Goddard Spaceflight Center, Greenbelt, MD, USA*

^c*Science Systems and Applications Inc., Lanham, MD, USA*

^d*Columbia University, New York, NY, USA*

^e*University of Tsukuba, Tsukuba, Japan*

^f*Jet Propulsion Laboratory, California Institute of Technology, Pasadena, CA, USA*

^g*USDA ARS Hydrology and Remote Sensing Laboratory, Beltsville, MD, USA*

^h*Instituto Hispano Luso de Investigaciones Agrarias (CIALE), Universidad de Salamanca, Salamanca, Spain*

ⁱ*Agriculture and Agri-food Canada, Ottawa, Ontario, Canada*

^j*Comisión Nacional de Actividades Espaciales (CONAE), Buenos Aires, Argentina*

^k*Department of Civil Engineering, Monash University, Clayton, Victoria, Australia*

^l*Centre d'Etudes Spatiales de la Biosphère (CESBIO-CNRS, CNRS, IRD, Université Toulouse III), Toulouse, France*

^m*University of Texas at Austin, TX, USA*

ⁿ*USDA ARS Southwest Watershed Research Center, Tucson, AZ, USA*

Abstract

A Neural Network (NN) algorithm was developed to estimate global surface soil moisture for April 2015 to March 2017 with a 2-3 day repeat frequency using passive microwave observations from the Soil Moisture Active Passive (SMAP) satellite, surface soil temperatures from the NASA Goddard Earth Observing System Model version 5 (GEOS-5) land modeling system, and Moderate Resolution Imaging Spectroradiometer-based vegetation water content. The NN was trained on GEOS-5 soil moisture target data, making the NN estimates consistent with the GEOS-5 climatology, such that they may ultimately be assimilated into this model without further bias correction. Evaluated against in

*Corresponding author

Email address: jana.kolassa@nasa.gov (J. Kolassa)

situ soil moisture measurements, the average unbiased root mean square error (ubRMSE), correlation and anomaly correlation of the NN retrievals were 0.037 m^3m^{-3} , 0.70 and 0.66, respectively, against SMAP core validation site measurements and 0.026 m^3m^{-3} , 0.58 and 0.48, respectively, against International Soil Moisture Network (ISMN) measurements. At the core validation sites, the NN retrievals have a significantly higher skill than the GEOS-5 model estimates and a slightly lower correlation skill than the SMAP Level-2 Passive (L2P) product. The feasibility of the NN method was reflected by a lower ubRMSE compared to the L2P retrievals as well as a higher skill when ancillary parameters in physically-based retrievals were uncertain. Against ISMN measurements, the skill of the two retrieval products was more comparable. A triple collocation analysis against Advanced Microwave Scanning Radiometer 2 (AMSR2) and Advanced Scatterometer (ASCAT) soil moisture retrievals showed that the NN and L2P retrieval errors have a similar spatial distribution, but the NN retrieval errors are generally lower in densely vegetated regions and transition zones.

Keywords: soil moisture remote sensing, SMAP, data assimilation, microwave radiometer

1. Introduction

Soil moisture is a key variable for many surface and boundary layer processes, such as the coupling of the water and energy cycles (*Seneviratne et al., 2006; Gentile et al., 2011; Bateni and Entekhabi, 2012*) or the partitioning of precipitation into runoff and infiltration (*Philip, 1957; Corradini et al., 1998; Assouline, 2013*). Soil moisture is also a key determinant of the carbon cycle (*McDowell, 2011; Sevanto et al., 2014; Jung et al., 2017*). The importance of soil moisture has been recognized by the World Meteorological Organization by

9 naming it an Essential Climate Variable (*GCOS*, 2009) and thus encouraging
10 efforts to obtain better soil moisture observations, which is challenging because
11 of its high variability both in space and time.

12 One avenue to obtain observations of soil moisture is through satellite instru-
13 ments that provide global observations with a relatively short revisit period of
14 2-3 days. In particular, L-band (1.4 GHz) microwave instruments exhibit a high
15 sensitivity to soil moisture in the top ~ 5 centimeters of the soil in sparsely to
16 moderately vegetated areas. This has led to the launch of two L-band satellite
17 missions to observe soil moisture, the European Soil Moisture and Ocean Salin-
18 ity (SMOS) mission in 2009 (*Kerr et al.*, 2010) and the NASA Soil Moisture
19 Active Passive (SMAP) mission (*Entekhabi et al.*, 2010) in 2015.

20 Traditionally, satellite soil moisture retrievals from L-band (and other) sen-
21 sors are implemented through the inversion of Radiative Transfer Models (RTMs)
22 (e.g. *Owe et al.* (2001); *Kerr et al.* (2012); *O'Neill et al.* (2015)), which explic-
23 itly formulate the physical relationships linking surface soil moisture to satellite
24 brightness temperature observations. The RTM inversion technique is used to
25 produce the official SMOS and SMAP retrieval products, and is able to provide
26 high quality soil moisture estimates (*Al Bitar et al.*, 2012; *Chan et al.*, 2016b;
27 *Colliander et al.*, 2017) with a typical latency of 12 to 24 hours. However, this
28 approach requires accurate knowledge of the physical relationships between the
29 surface state and the satellite observations as well as their associated parame-
30 ters, which are often empirically estimated and thus uncertain. Moreover, RTM
31 inversions also require explicit information on other surface states, including

32 surface soil temperature and vegetation, and are thus typically ill-posed prob-
33 lems. Additionally, for time critical applications, such as near real time flood
34 prediction or soil moisture assimilation into weather prediction models, retrieval
35 products with a shorter latency are required.

36 Data assimilation provides another option to generate improved soil moisture
37 estimates through the merging of satellite and model information, and can yield
38 soil moisture estimates that are of higher quality than estimates from satellite
39 observations or models alone (e.g. *Entekhabi et al. (1994); Walker and Houser*
40 *(2001); Liu et al. (2011); Lahoz and De Lannoy (2014)*). For soil moisture
41 assimilation, the observations and model estimates have to be unbiased with
42 respect to each other, which is typically achieved by locally matching the mean
43 and variability of the satellite observations to those of the model (*Reichle and*
44 *Koster, 2004*). While this satisfies the requirements of the assimilation system,
45 it has the side effect of removing some independent information in the satellite
46 observations. Given the high quality of soil moisture observations from SMOS
47 and SMAP this is undesirable.

48 As an alternative to RTM inversions, statistical Neural Network (NN) re-
49 trieval algorithms have been successfully implemented for a number of sensors
50 in recent years (*Aires et al., 2005; Chai et al., 2009; Kolassa et al., 2013, 2016;*
51 *Rodriguez-Fernández et al., 2015; Santi et al., 2016*). Instead of explicitly for-
52 mulating physical relationships, NNs are calibrated on a sample of satellite ob-
53 servations and corresponding soil moisture estimates (the target data) to model
54 the global statistical relationship between the satellite observations and surface

55 soil moisture. As a result, NN retrievals can offer several general advantages
56 over traditional RTM inversions. First, they do not require an explicit param-
57 eterization of physical relationships and are thus not affected by errors in our
58 knowledge of these relationships or their parameters. Second, after a one-time
59 calibration, NNs are computationally extremely efficient and can provide soil
60 moisture estimates almost immediately after arrival of the instrument data,
61 thereby shortening the latency. Third, training a NN non-locally on target data
62 from a model, yields NN retrievals that are globally unbiased with respect to
63 the model, with spatial and temporal patterns that are driven by the satellite
64 observations (e.g. *Jimenez et al. (2013)*; *Kolassa et al. (2016)*; *Alemohammad et*
65 *al. (2017)*). This may reduce the need for bias correction prior to an assimilation
66 and at the same time retain more of the independent information contained in
67 the spatial and temporal patterns of the satellite observations.

68 In this study, we develop the first NN algorithm to retrieve global surface
69 soil moisture from SMAP observations. The motivation for this work is two-
70 fold. First, we investigate statistical retrieval techniques as a possible alterna-
71 tive or supplement to the existing physically-based SMAP retrieval algorithms.
72 Since statistical techniques require less ancillary data and are subject to differ-
73 ent algorithm-related errors than physically-based retrievals, NN retrievals may
74 provide useful information where and when RTMs are known to be uncertain.
75 For SMOS, the NN technique has been successfully implemented (*Rodriguez-*
76 *Fernández et al., 2015*). However, it is not obvious that a NN for SMAP will
77 work equally well, given the differences between SMOS and SMAP in the ob-

78 serving geometry (multiple vs. single incidence angle) and instrument error
79 characteristics (*De Lannoy et al.*, 2015). Second, we aim to investigate the
80 potential of statistical techniques to generate a soil moisture product with char-
81 acteristics beneficial to SMAP soil moisture assimilation. The NN algorithm
82 retrieves soil moisture in the climatology of the target model and thus may
83 reduce the need for bias correction prior to data assimilation. In a follow-on
84 study, we will investigate whether this results in a more efficient use of SMAP
85 observations during data assimilation.

86 The NN retrieval algorithm is trained with SMAP brightness temperatures
87 and two ancillary datasets as inputs, and with target data from the NASA God-
88 dard Earth Observing System version 5 (GEOS-5) model (section 2). Using the
89 trained NN, we compute global estimates of volumetric surface soil moisture
90 for the period April 2015 to March 2017 and evaluate them using a number of
91 different metrics and techniques (section 3). We compare the SMAP NN soil
92 moisture estimates to the target GEOS-5 model soil moisture to identify the in-
93 dependent information provided by the SMAP observations that can potentially
94 inform the model during data assimilation (section 4.1). Next, we assess the
95 SMAP NN retrievals against independent in situ measurements and compare
96 their skill to that of the SMAP Level-2 passive (L2P) retrieval product and the
97 GEOS-5 model soil moisture (section 4.2). Finally, we assess the global error
98 distributions of the SMAP NN, GEOS-5 and SMAP L2P products using a triple
99 collocation (TC) analysis in conjunction with soil moisture retrievals based on
100 observations from the Advanced Microwave Scanning Radiometer 2 (AMSR2)

101 and the Advanced Scatterometer (ASCAT), which have independent errors with
102 respect to the SMAP and GEOS-5 products (section 4.3).

103 **2. Datasets**

104 *2.1. Neural Network Inputs and Target Datasets*

105 *2.1.1. SMAP Observations*

106 The main input to the NN soil moisture retrieval algorithm are the SMAP
107 brightness temperatures. SMAP was launched in January 2015 and is equipped
108 with an L-band (1.4 GHz) radiometer observing on four different channels, hor-
109 izontal and vertical polarization as well as the 3rd and 4th Stokes' parameter.
110 SMAP is in a sun-synchronous, near-circular orbit with equator crossings at 6
111 AM and 6 PM local time and a revisit time of 2-3 days (*Entekhabi et al., 2010*).
112 Brightness temperature data have been collected since 31 March 2015.

113 For our NN retrieval product we use SMAP Level-1C brightness temper-
114 atures (*Chan et al., 2016a*) for the April 2015 to March 2017 period. The
115 data are provided on the 36-km resolution Equal-Area Scalable Earth version
116 2 (EASEv2) grid (*Brodzik et al., 2012*) as daily half-orbit files. We only use
117 observations from the 6 AM overpass, in order to minimize observation errors
118 due to Faraday rotation and the difference between the soil and canopy tem-
119 peratures (*Entekhabi et al., 2010; O'Neill et al., 2015*). A test of different input
120 combinations indicated that using data from all four SMAP channels as in-
121 puts to the retrieval algorithm yielded the best NN retrieval performance (not
122 shown). While the 3rd and 4th Stokes' parameters are not directly sensitive to

123 soil moisture, including them as inputs helps the NN algorithm to distinguish
124 between different observing conditions and thus determine the weight for a given
125 brightness temperature observation.

126 *2.1.2. GEOS-5 Model Surface Soil Moisture and Temperature*

127 The model soil moisture estimates used here are generated using the GEOS-
128 5 Catchment land surface model (*Koster et al., 2000; Ducharne et al., 2000*).
129 The Catchment model version used in this study is very similar to that of the
130 SMAP Level-4 Soil Moisture (L4.SM) version 2 system (*Reichle et al., 2015,*
131 *2016, 2017b* (in press), but SMAP brightness temperature observations are not
132 assimilated. The surface meteorological forcing data were provided at 0.25°
133 resolution by the GEOS-5 Forward Processing atmospheric data assimilation
134 system (*Lucchesi, 2013*). The GEOS-5 precipitation forcing data were cor-
135 rected using global, daily, 0.5° resolution, gauge-based observations from the
136 Climate Prediction Center Unified (CPCU) product, which have been scaled to
137 the Global Precipitation Climatology Project (GPCP) v2.2 pentad precipita-
138 tion product climatology (*Reichle and Liu, 2014; Reichle et al., 2017a,b*). The
139 GEOS-5 background precipitation was also scaled to the GPCP v2.2 climatol-
140 ogy. Output fields were produced as 3-hourly time averages and provided on
141 the 9-km EASEv2 grid.

142 In this study, we use two model output fields: (1) the surface soil moisture
143 (0-5 cm soil layer) and (2) the surface soil temperature (0-10 cm soil layer). The
144 GEOS-5 soil moisture fields served as target data in the NN training (section
145 3.1) and were also used in the evaluation phase to assess the skill of the NN

146 retrieval compared to that of the target model. The surface soil temperature
147 data were used as an input to the retrieval algorithm to account for the surface
148 soil temperature contribution to the observed brightness temperatures (section
149 3.1). Using surface soil temperature estimates from the target model potentially
150 introduces some of the GEOS-5 spatial patterns into the NN estimates and could
151 lead to model dependency issues during a later assimilation of the NN estimates
152 into the GEOS-5 model. The same would be true, however, for the assimilation
153 of the SMAP L2P product, which also uses GEOS-5 ancillary soil temperatures
154 (section 2.2.1). We assume here that the canopy temperature and surface soil
155 temperature are in equilibrium for the 6 AM (local time) SMAP observations
156 used here, so only a single temperature estimate is required. The surface soil
157 temperature data were also used in the data quality control to identify frozen
158 soil conditions (section 2.3).

159 *2.2. Validation Datasets*

160 *2.2.1. SMAP Level-2 Passive Retrievals*

161 The SMAP L2P soil moisture retrieval product uses SMAP radiometer Level-
162 1C brightness temperatures to provide soil moisture estimates on the 36-km EA-
163 SEv2 grid as daily half-orbit files. The retrieval algorithm is based on a physical
164 tau-omega model (*Wigneron et al., 1995; O'Neill et al., 2015*) to isolate the soil
165 emission from the total observed surface emission (soil and vegetation) and to
166 subsequently convert it into a soil moisture estimate through the use of soil
167 emission and mixing models. The surface soil temperature data required by
168 the tau-omega model are provided by the quasi-operational GEOS-5 Forward

169 Processing system (*Lucchesi, 2013*) with a 0.25° resolution. The tau-omega
170 model also requires information on the vegetation water content (VWC), which
171 is estimated from a climatology of the Normalized Difference Vegetation Index
172 based on Moderate Resolution Imaging Spectroradiometer (MODIS) observa-
173 tions using an empirical relationship established from prior investigations. No
174 retrieval is performed for frozen soil conditions based on GEOS-5 surface soil
175 temperature. Soil moisture retrievals are flagged as ‘not recommended’ when
176 the VWC within the satellite footprint exceeds 5 kg m^{-2} (*O’Neill et al., 2015*).

177 In this study, we use version 4 of the L2P ‘baseline’ soil moisture estimates
178 derived from the SMAP morning (6 AM) overpass vertical polarization bright-
179 ness temperatures (*O’Neill et al., 2016*). Only data points flagged as having the
180 ‘recommended’ retrieval quality were used.

181 *2.2.2. AMSR2 and ASCAT Soil Moisture Retrievals*

182 The Advanced Multichannel Scanning Radiometer 2 (AMSR2) is a multi-
183 channel passive microwave satellite instrument that has been collecting data
184 since July 2012. AMSR2 measures brightness temperatures at frequencies rang-
185 ing from 6.9 GHz to 89 GHz with a revisit time of approximately 2 days and
186 equator crossings at 1.30 AM and 1.30 PM local time (*Kasahara et al., 2012*).

187 Here we use the Japan Aerospace Exploration Agency AMSR2 soil moisture
188 product computed from the 10.7 GHz and 36.5 GHz vertical and horizontal
189 polarization brightness temperatures (*Maeda and Taniguchi, 2013*). The data
190 are provided as daily estimates of volumetric surface soil moisture on a grid
191 with $0.1^\circ \times 0.1^\circ$ resolution spacing.

192 The Advanced Scatterometer (ASCAT) (*Figa-Saldaña et al.*, 2002) is an
193 active microwave satellite instrument aboard the MetOp satellites, which have
194 been collecting data since 2006. ASCAT measures surface backscatter at C-
195 band (5.3 GHz) with a revisit time of 1-2 days and equator crossings at 9.30
196 AM and 9.30 PM.

197 Here we use the ASCAT surface soil moisture product developed by *Wagner*
198 *et al.* (2013). The data are provided in units of surface degree of saturation
199 with a sampling distance of 12.5 x 12.5 km and were converted into estimates
200 of volumetric surface soil moisture using the soil porosity data of *Reynolds et*
201 *al.* (2000).

202 Despite being posted on finer resolution grids, the spatial resolution of the
203 AMSR2 and ASCAT observations is very similar to the SMAP 36-km resolution.

204 2.2.3. *In Situ Measurements*

205 *SMAP Core Validation Sites.* The SMAP core validation sites (referred to here
206 as ‘core sites’) represent locally dense networks of in situ soil moisture measure-
207 ments that are specifically designed for the calibration and validation of SMAP
208 soil moisture products (*Colliander et al.*, 2017). Each site features an array of
209 soil moisture sensors to represent the different spatial scales of the SMAP prod-
210 ucts (3 km, 9 km and 36 km). The measurements from each site’s sensors are
211 combined into an area-weighted average to yield one soil moisture time series
212 per site that is representative of a 36-km satellite grid cell.

Table 1: Overview of the SMAP Cal/Val core sites. Shown are (from left to right) the site name, reference pixel ID (RPID), location, climate, land cover and the average number of sensors that contribute to the reference pixel average. Soil moisture is measured at 5 cm depth or over the top 5 cm. (*Colliander et al., 2017*)

Site (abbreviation)	RPID	location	climate	land cover	number of sensors
REMEDIHUS (RM)	03013602	Spain	temperate	croplands	14
Reynolds Creek (RC)	04013601	USA (Idaho)	arid	grasslands	5
Yanco (YC)	07013601	Australia	arid	croplands	26
Carman (CM)	09013601	Canada	cold	croplands	19
Twente (TW)	12043602	Holland	temperate	croplands / natural mosaic	9
Walnut Gulch (WG)	16013603	USA (Arizona)	arid	shrub open	20
Little Washita (LW)	16023602	USA (Oklahoma)	temperate	grasslands	16
Fort Cobb (FC)	16033602	USA (Oklahoma)	temperate	grasslands	12
Little River (LR)	16043602	USA (Georgia)	temperate	croplands / natural mosaic	19
South Fork (SF)	16073602	USA (Iowa)	cold	croplands	18
Monte Buey (MB)	19023601	Argentina	temperate	croplands	10
Kenaston (KN)	27013601	Canada	cold	croplands	26
TxSON (TX)	48013601	USA (Texas)	temperate	grasslands	32
Mahasri (MH)	53013601	Mongolia	cold	grasslands	5

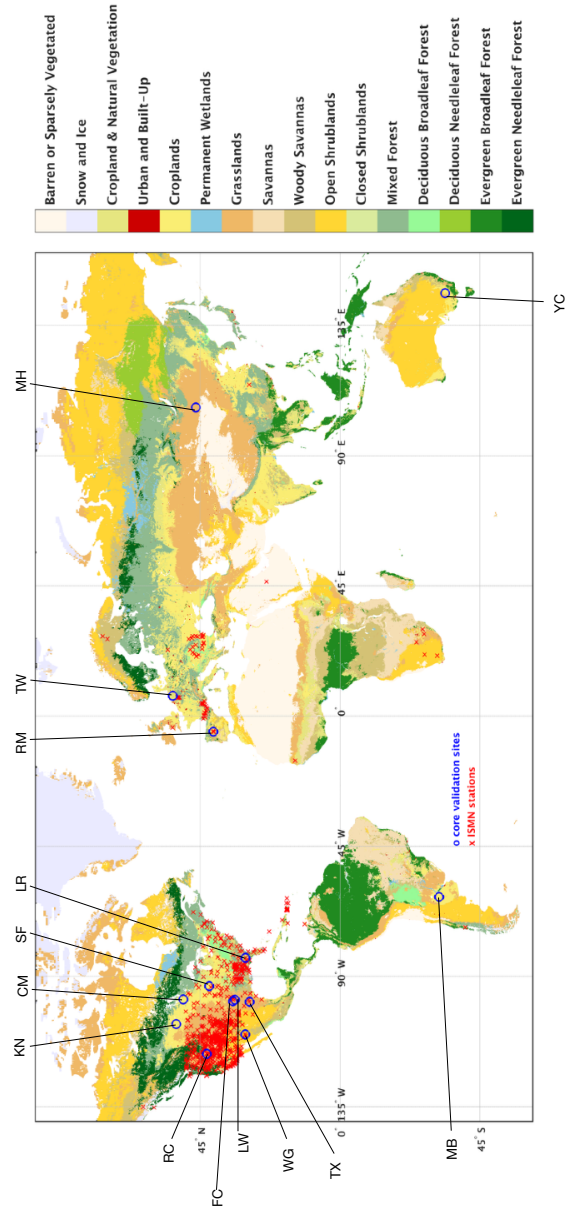


Figure 1: Location of the SMAP core validation sites (blue circles) and ISMN stations (red crosses). The background shows the dominant International Geosphere-Biosphere Program (IGBP, (Belward *et al.*, 1999)) land cover class for each location.

213 Table 1 summarizes the main characteristics of the 36-km core sites used
214 here. Out of the 14 locations, nine are in North America, two in Europe, and
215 one each in Asia, Australia and South America. The sites represent a range
216 of different climatic conditions and land cover types, and the average number
217 of sensors that contribute to the 36-km reference pixel data ranges between
218 5 and 32. Figure 1 shows the distribution of the SMAP core sites and their
219 corresponding dominant land cover.

220 *International Soil Moisture Network (ISMN).*

Table 2: Overview of the ISMIN (Dorigo et al., 2011). Shown are the location, number of stations per network and the network-specific reference.

Network	location	# stations	reference
Dahra	Senegal	1	(Tagesson et al., 2015)
FMI	Finland	27	(Dorigo et al., 2011)
iRON	USA	6	(Taylor et al., 2015)
PBO H2O	USA	161	(Larson et al., 2008)
REMEDIHUS	Spain	24	(Sanchez et al., 2012)
RSMN	Romania	20	(Dorigo et al., 2011)
SCAN	USA	181	(Schaefer et al., 2007)
SMOSMANIA	France	21	(Cabnet et al., 2007)
SNO TEL	USA	441	(Leavesley et al., 2008)
SOILSCAPE	USA	171	(Moghaddam et al., 2016)
USCRN	USA	115	(Diamond et al., 2013)

221 We further evaluate the NN retrieval product against independent in situ soil
222 moisture measurements from the International Soil Moisture Network (ISMN),
223 a database of soil moisture networks hosted at the Technical University (TU)
224 of Vienna (*Dorigo et al.*, 2011) and referred to here as the ‘sparse networks’.
225 We used only ISMN networks that are not part of the SMAP core sites (Table
226 2). The REMEDHUS network comprises a different set of sensors for the core
227 site and as a sparse network and thus appears for both in situ data types. The
228 measurement depth, repeat frequency, coverage, station density and measure-
229 ment method depend on the contributing network. The number of stations in
230 each network ranges between 1 and 441 (Table 2), but - unlike for the core sites
231 - there is typically only one sensor per 36-km grid cell. That is, the ISMN mea-
232 surements are not necessarily representative of the spatial scale of the satellite
233 observations. Figure 1 shows the spatial distribution of the ISMN stations and
234 the dominant land cover at each location.

235 For two of the ISMN networks, SCAN (*Schaefer et al.*, 2007) and USCRN
236 (*Diamond et al.*, 2013), the data were already available in-house and had been
237 subjected to additional quality control as described in *De Lannoy et al.* (2014)
238 and (*Reichle et al.*, 2015b) (their Appendix C). Hence, the in-house data were
239 used for SCAN and USCRN instead of the data provided through the ISMN. As
240 a result, more reliable metrics could be estimated for these two sparse networks.

241 *2.3. Data Preprocessing*

242 *2.3.1. Satellite Observations and Model*

243 We co-located all datasets spatially and temporally, using the 36-km EASEv2
244 grid and the SMAP morning (6 AM) overpass times as a reference. The GEOS-5,
245 AMSR2 and ASCAT data were aggregated from their higher-resolution native
246 grids to the 36-km EASEv2 grid using simple averaging. The temporal co-
247 location was implemented by using the GEOS-5 3-hourly average that includes
248 the SMAP morning overpass for a given location and day. For the AMSR2 and
249 ASCAT retrieval products, only data from their night-time/morning overpasses
250 for the same day - at 1.30 AM and 9.30 AM, respectively - were used since
251 these are closest in time to the SMAP overpass at 6 AM. Likewise, for the L2P
252 retrievals we used only the morning overpass estimates, and no regridding was
253 required because the SMAP-based NN and L2P products are provided on the
254 same 36-km EASEv2 grid.

255 We additionally applied several quality control steps to the satellite and
256 model data sets to identify and exclude conditions in which a soil moisture re-
257 trieval was not feasible. Using the GEOS-5 surface soil temperature, we excluded
258 times and locations with a surface soil temperature below 1°C. The MODIS-
259 based VWC estimates provided with the L2P data were used to exclude times
260 and locations with a VWC higher than 5 kg m⁻², where the SMAP radiometer
261 is not expected to provide reliable retrievals. Finally, we excluded all pixels
262 within 72 km of a water body - defined as a grid cell with a water fraction in
263 excess of 5% according to the GEOS-5 land mask - to mitigate the impact of

264 water bodies, as their low brightness temperatures cause erroneously high soil
265 moisture retrievals (*O'Neill et al.*, 2015).

266 *2.3.2. In Situ Data*

267 The core site measurements are representative of the 36-km spatial resolution
268 of the retrievals and the aggregated model, however, the geographical center of
269 the in situ sensors for a given reference pixel does not generally coincide with
270 the EASEv2 grid cell center of the satellite and model products. Similarly,
271 the location of a (single point) ISMN measurement is typically offset from the
272 center of a EASEv2 grid cell. To account for this, the retrieval and (aggregated)
273 model soil moisture were linearly interpolated to the in situ location using data
274 from the nearest EASEv2 grid cell and its 8 surrounding neighbors, requiring a
275 minimum of 4 data points. Where applicable, ISMN measurements located in
276 the same EASEv2 grid cell were averaged and their average location was used
277 for the interpolation. For each day, the in situ measurement closest in time and
278 within a 3 hour window of the SMAP overpass was used.

279 Using the GEOS-5 surface temperature for the ISMN measurements and the
280 in situ surface soil temperature observations for the core site measurements, the
281 in situ data were screened for (nearly) frozen soil conditions by applying the
282 same 1°C threshold that was used for the satellite and model data.

283 **3. Methodology**

284 *3.1. Neural Network Retrieval Algorithm*

285 In this study we use a NN approach to retrieve global surface soil mois-
286 ture with a 2-3 day repeat using SMAP brightness temperatures, GEOS-5 soil
287 temperatures and the MODIS-based VWC climatology that is used in the gener-
288 ation of the SMAP L2P product. The NN retrieval algorithm is first calibrated
289 (trained) using a subset of the available SMAP and model data to determine the
290 statistical relationship between the satellite observations and surface soil mois-
291 ture. Once calibrated, the trained NN is used to retrieve surface soil moisture
292 from the entire set of satellite observations.

293 *3.1.1. Neural Network Architecture*

294 A neural network is a group of computational nodes arranged in a layered
295 and inter-connected architecture. Figure 2 shows a schematic of a basic NN for
296 soil moisture retrievals. The NN used here consists of 3 layers: (1) an input layer
297 that receives the satellite observations and ancillary inputs, (2) one hidden layer,
298 and (3) an output layer that produces the soil moisture estimates. This archi-
299 tecture is sufficient to approximate any continuous function (*Cybenko, 1989*).
300 The inputs for the SMAP NN retrieval algorithm are the observations from the
301 four SMAP channels, the GEOS-5 surface soil temperature and the MODIS-
302 based VWC estimates. The output from the NN algorithm is an estimate of the
303 volumetric surface soil moisture.

304 While the number of neurons in the input and output layers is determined by

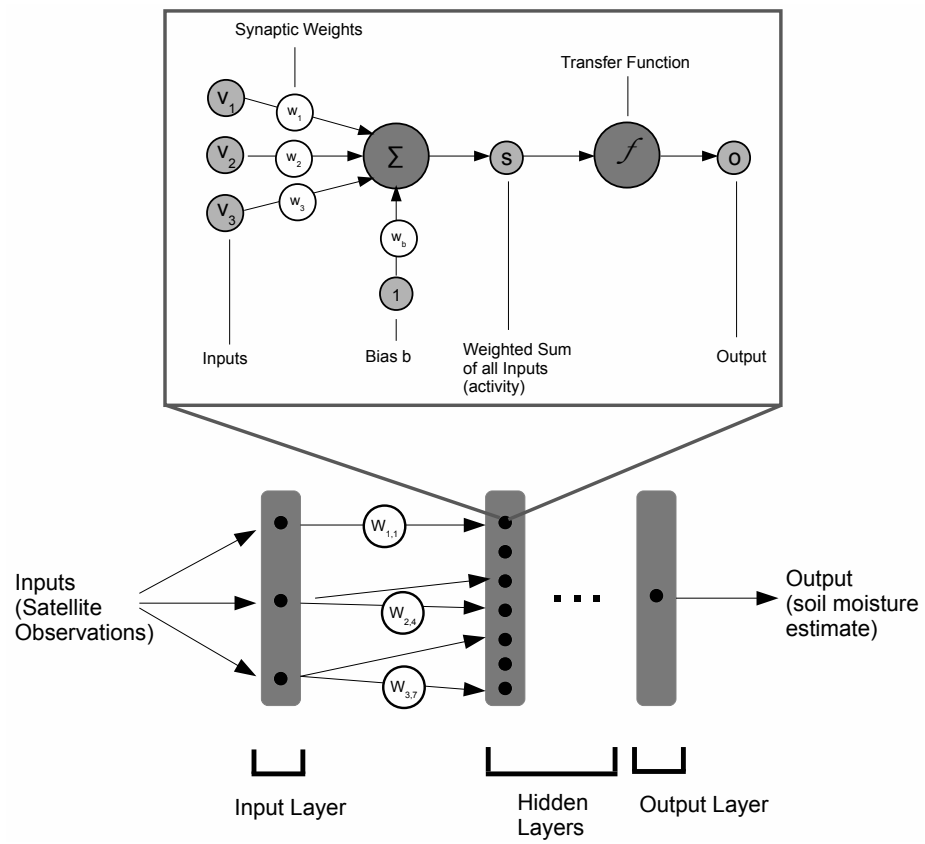


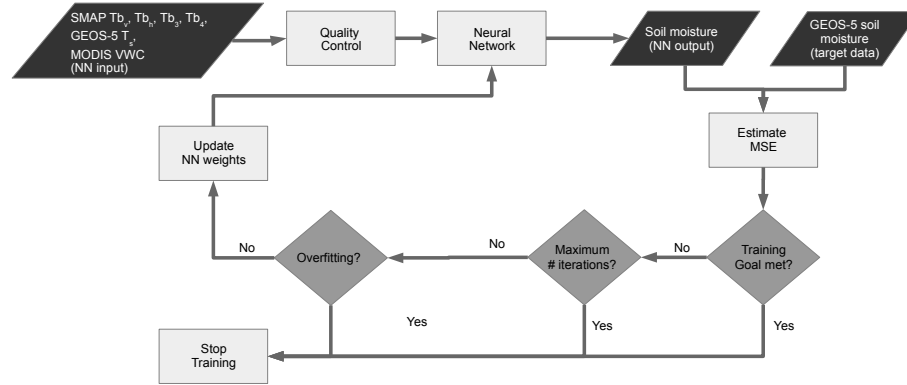
Figure 2: Schematic of a neural network with close-up of a single neuron (adapted from Kolassa (2013)).

305 the number of input and output variables (here, 6 for the input layer and 1 for
306 the output layer), the optimal number of neurons in the hidden layer depends on
307 the problem complexity. We found that for this study 15 hidden layer neurons
308 constituted the lowest number of neurons that was able to converge to a solution
309 during the NN training. We use a fully connected feed-forward network, in which
310 all neurons from one layer are connected to all neurons in the next layer. These
311 connections are assigned weights - the synaptic weights - used by each neuron
312 to compute a weighted sum of all its input plus a bias before applying a transfer
313 function. Neurons in the input and output layers use a linear transfer function,
314 while hidden layer neurons use the typical tangent-sigmoid transfer function.

315 *3.1.2. Neural Network Training*

316 In order to determine the statistical function that relates the NN input
317 data, including the satellite brightness temperature observations, to surface soil
318 moisture, the NN is calibrated on a sample set of NN inputs and coincident soil
319 moisture estimates (the target data), together referred to as the training data.
320 This process is referred to as the NN training and is schematically illustrated
321 in Figure 3 (a). To generate a training dataset representative of all expected
322 conditions, we used the first year (April 2015 - March 2016) of our study period
323 for NN training. The second year (April 2016 - March 2017) of the study
324 period was used for the evaluation presented in sections 4.1 and 4.2. Model
325 soil moisture estimates from GEOS-5 are used as the target data, because (1)
326 the model estimates have a similar resolution as the satellite observations while
327 providing complete spatio-temporal coverage and (2) training on a model yields

(a) NN Training



(b) Soil Moisture Estimation



Figure 3: The two phases of the NN soil moisture retrieval approach. (a) NN training and (b) soil moisture estimation using the trained network. NN inputs include the SMAP brightness temperatures at vertical and horizontal polarization (Tb_v and Tb_h), the 3rd and 4th Stokes' parameters (Tb_3 and Tb_4), the GEOS-5 surface soil temperature (T_s), and the MODIS-based vegetation water content (VWC).

328 NN estimates in the global model climatology, which could be beneficial for a
329 later assimilation of the retrieved soil moisture.

330 The total training dataset is split into three subsets - the calibration, val-
331 idation and test data - by sampling the total dataset. The calibration data
332 constitute 60% of the total training data and are used to optimize the NN
333 synaptic weights (Note: In the literature these data are often referred to as
334 'training data'. In order to avoid confusion with the total training dataset, we
335 have decided to use the term 'calibration data' instead). The validation data
336 constitute 20% of the total training data and are used to detect over-fitting of

337 the NN weights (see below). These are part of the training data and should not
338 be confused with the independent evaluation data used in sections 4.1 and 4.2 to
339 assess the SMAP NN retrieval quality. The test data constitute the remaining
340 20% of the training data and are used to assess the NN fit.

341 The NN training is non-localized, meaning that one NN is fitted to a global
342 training dataset that contains data from the entire training period (April 2015
343 - March 2016). Furthermore, no information regarding the location and acqui-
344 sition time of the training points is provided to the NN. The NN training thus
345 essentially involves an association of the same sets of input values (that is, the
346 same brightness temperatures, Stokes' parameters, and ancillary data) with the
347 mean value of the corresponding target soil moisture data. If, for example, the
348 target data in a specific region overestimate the soil moisture, they will appear
349 as outliers in the NN training, and the NN will thus not inherit such regional
350 errors (e.g., (*Jimenez et al.*, 2013)). As a result, the spatial and temporal pat-
351 terns of the NN estimates are mostly driven by the input satellite observations.
352 Moreover, the NN estimates match the global (single-value) mean and variabil-
353 ity of the target data, but mean differences in the spatial patterns between the
354 satellite observations and the model estimates are retained. These remaining
355 local biases could represent an issue during an assimilation of the NN product.
356 Further investigation will be needed to determine whether the disadvantage of
357 local biases in the assimilation is outweighed by the benefit of retaining more of
358 the independent information in the assimilated SMAP observations.

359 The training itself consists of an iterative optimization of the NN synaptic

360 weights to minimize the error between the NN output and the target data (Fig-
361 ure 3 (a)). Three different scenarios cause the NN training to stop. First, the
362 training is stopped when the mean squared error between the NN outputs and
363 the target data is less than $0.001 \text{ m}^3\text{m}^{-3}$ and the training goal is met. Second,
364 the training is stopped when the NN training does not converge to a solution
365 after a maximum number of iterations - set here at 1000. Third, training is
366 stopped when over-fitting of the NN weights to the calibration data is detected.
367 For this, the error between NN estimates computed from the validation input
368 data and the validation model soil moistures is estimated upon each iteration. A
369 divergence of the validation estimates from the corresponding validation model
370 soil moisture indicates an over-fitting of the NN weights to the calibration data
371 and a loss of the NN's generalization ability. When such a divergence is de-
372 tected for six subsequent iterations, the training is stopped and the weights
373 from the last iteration before the occurrence of the divergence are used as the
374 final solution.

375 Here we use a Levenberg-Marquardt training algorithm (*Levenberg, 1944;*
376 *Marquardt, 1963*) and apply an error back-propagation approach (*Rumelhart*
377 *and Chauvin, 1995*) to update the weights. The Levenberg-Marquardt algorithm
378 stops when a local minimum is found and thus does not permit a full exploration
379 of the error surface. To account for this, the NN training is repeated four
380 times, using a different random initialization for the NN weights (and thus a
381 different starting point on the error surface) each time. This corresponds to four
382 repetitions of the training process illustrated in Figure 3 (a). After the training

383 is stopped, we compute the root mean square error (RMSE) between the NN
384 estimates computed from the test data and the corresponding test model soil
385 moistures to assess the NN fit. The NN with the lowest RMSE error out of the
386 four repetitions is then retained as the optimal NN and used to generate the
387 soil moisture retrieval product.

388 The trained NN is used to compute global estimates of volumetric soil mois-
389 ture from the complete set of satellite observations and ancillary data (Figure
390 3 (b)). The soil moisture estimates are computed for the period April 2015 to
391 March 2017 and include both the training data (first year) and the evaluation
392 data (second year) that was not used in the training phase.

393 *3.2. Evaluation Metrics*

394 As part of the NN retrieval development, we evaluate our retrieval product
395 against in situ soil moisture measurements and assess its fit with respect to the
396 target model. To quantify different aspects of the retrieval product and model
397 skill, we use the correlation R , anomaly correlation R_{anom} and unbiased root
398 mean square error $ubRMSE$. These metrics have been chosen, because they
399 evaluate different aspects of the retrieval products and provide complementary
400 information on the product skill. Additionally, they are well-established for
401 the evaluation of soil moisture retrievals (*Al Bitar et al., 2012; Albergel et al.,*
402 *2013; Chan et al., 2016b; Colliander et al., 2017*). The evaluation metrics are
403 computed with respect to the model soil moisture estimates (section 4.1) and
404 in situ measurements (section 4.2).

405 The correlation (R) estimates the ability to capture soil moisture variations

406 at all time scales and is computed as the Pearson correlation coefficient between
407 the raw soil moisture and reference data time series in each location. The
408 anomaly correlation (R_{anom}) estimates the ability to capture individual drying
409 and wetting events and is computed similarly to the correlation, but using the
410 anomaly time series, with the anomalies defined with respect to the 30-day
411 moving average centered on the current day. The $ubRMSE$ measures the RMSE
412 excluding the bias and is computed after removing the long-term mean from the
413 soil moisture and reference data time series in each location. When assessing
414 the fit between the NN retrieval product and its target model (section 4.1),
415 we use the term unbiased root mean square *difference* ($ubRMSD$) to indicate
416 that the target model is not considered the truth in this case. Rather, the
417 $ubRMSD$ simply aims to identify differences between the observed and modeled
418 soil moistures.

419 When evaluating the skill of the retrieval and model products against in situ
420 measurements, only data points common to all four datasets (i.e., the NN and
421 L2P retrievals, GEOS-5 model estimates, and in situ measurements) contributed
422 to the metric calculations, with a minimum of 30 data points required. For the
423 evaluation against ISMN data, we report the average metrics across all stations
424 in a network. Following the approach used by *De Lannoy and Reichle (2016)*,
425 we employ a k-means clustering to avoid a dominance of areas with a high
426 station density and to obtain realistic confidence intervals. The spatial extent
427 of each cluster is limited to 1° around its center. Additionally, we report average
428 metrics computed across all sites for the evaluation against core site data and

429 across all networks for the evaluation against the ISMN data, applying the same
430 clustering approach.

431 3.3. Triple Collocation Analysis

432 The evaluation of the NN retrieval product against in situ observations is
433 limited by the availability of the in situ measurements and thus only covers
434 a limited range of climate regions and land cover types. However, for most
435 applications, and in particular for data assimilation, retrieval error estimates
436 are required for every location. Here, we implement a triple collocation (TC)
437 analysis (*Stoffelen, 1998; McColl et al., 2014*) in order to compute a global map
438 of error estimates for the NN soil moisture product.

439 Triple collocation resolves the linear relationships between three independent
440 datasets of the same variable (here, soil moisture) in order to estimate the
441 errors in each dataset independent of a reference. It is a localized technique
442 that estimates the errors for all three datasets in each location independently,
443 yielding a map of error estimates. Several studies have successfully applied TC
444 to estimate soil moisture retrieval errors (e.g., *Scipal et al. (2008); Draper et*
445 *al. (2013); Su et al. (2014); Chen et al. (2016)*). Here, we use TC to estimate
446 the NN retrieval product errors and, for comparison, the errors of the GEOS-5
447 model and L2P soil moisture. However, one of the main assumptions of the TC
448 analysis is an independence of the errors in the three datasets that constitute
449 the triplet. In the case of the NN, GEOS-5 and L2P products this assumption
450 cannot be made, since the NN uses information from the GEOS-5 model while
451 the NN and L2P retrievals rely on the same satellite input data. We therefore

452 use the independent soil moisture retrieval products from AMSR2 and ASCAT
453 (section 2.2.2) to create three suitable triplets: [SMAP NN, AMSR2, ASCAT],
454 [GEOS-5, AMSR2, ASCAT] and [SMAP L2P, AMSR2, ASCAT]. This allows us
455 to derive error estimates for SMAP NN, GEOS-5 and SMAP L2P.

456 Following *McColl et al. (2014)* and *Draper et al. (2013)*, we apply the ex-
457 tended TC to the anomaly soil moisture time series (section 3.2) and compute
458 an error estimate in each location with at least 10 common data points in the
459 three contributing datasets. A bootstrapping approach with 100 samples is ap-
460 plied to ensure a robust error estimation. To mitigate the error dependence
461 on the (product- and location-specific) soil moisture variability, we estimate the
462 fractional error standard deviation (*Draper et al., 2013; Gruber et al., 2016*), de-
463 fined here as the error standard deviation divided by the soil moisture standard
464 deviation of the corresponding product in each location. The fractional error
465 standard deviation is an approximation of the noise-to-signal ratio, with values
466 below 1 indicating that the noise is smaller than the signal and values greater
467 than 1 indicating that the noise exceeds the signal.

468 **4. Results and Discussion**

469 *4.1. Neural Network Fit*

470 As a first assessment, we compare the NN soil moisture estimates to the
471 GEOS-5 modeled soil moisture used as the target data. The purpose of this is
472 to (1) assess the NN fit with respect to the target data over the training period,
473 (2) evaluate the NN’s ability to generalize beyond the training data and (3)

474 identify areas of disagreement between the SMAP driven NN estimates and the
475 model soil moisture. In such areas, an assimilation of the NN retrievals should
476 result in the largest changes to the model.

477 Over the training period, the domain average ubRMSD, correlation and
478 anomaly correlation between the NN and GEOS-5 soil moistures are 0.037
479 m^3m^{-3} , 0.60 and 0.53, respectively. These fit values are typical for daily NN
480 soil moisture retrievals (for example (*Kolassa et al.*, 2016)). For the NN train-
481 ing it is not desirable to obtain a perfect fit with respect to the target data,
482 since the non-localized calibration results in spatial and temporal patterns that
483 are driven by the satellite input observations and are thus expected to differ
484 from patterns in the target data (*Jimenez et al.*, 2013). Nevertheless, the fairly
485 high correlation and low ubRMSD values indicate that the SMAP based NN
486 soil moisture corresponds with the estimates generated by the model in most
487 regions.

488 To assess the NN's ability to generalize beyond the training dataset and to
489 investigate the spatial distribution of the differences between the NN estimates
490 and the GEOS-5 soil moisture, we also compared both datasets over the evalua-
491 tion period, i.e., using only data points that were not part of the training dataset.
492 Figure 4 shows maps of the ubRMSD, correlation, anomaly correlation and bias
493 between the NN estimates and the model soil moisture. Averaging across these
494 maps yields a ubRMSD, correlation and anomaly correlation of 0.037 m^3m^{-3} ,
495 0.61 and 0.55, respectively, which are similar to the average metrics obtained
496 for the training period and indicate that the NN is able to generalize beyond

497 the training dataset.

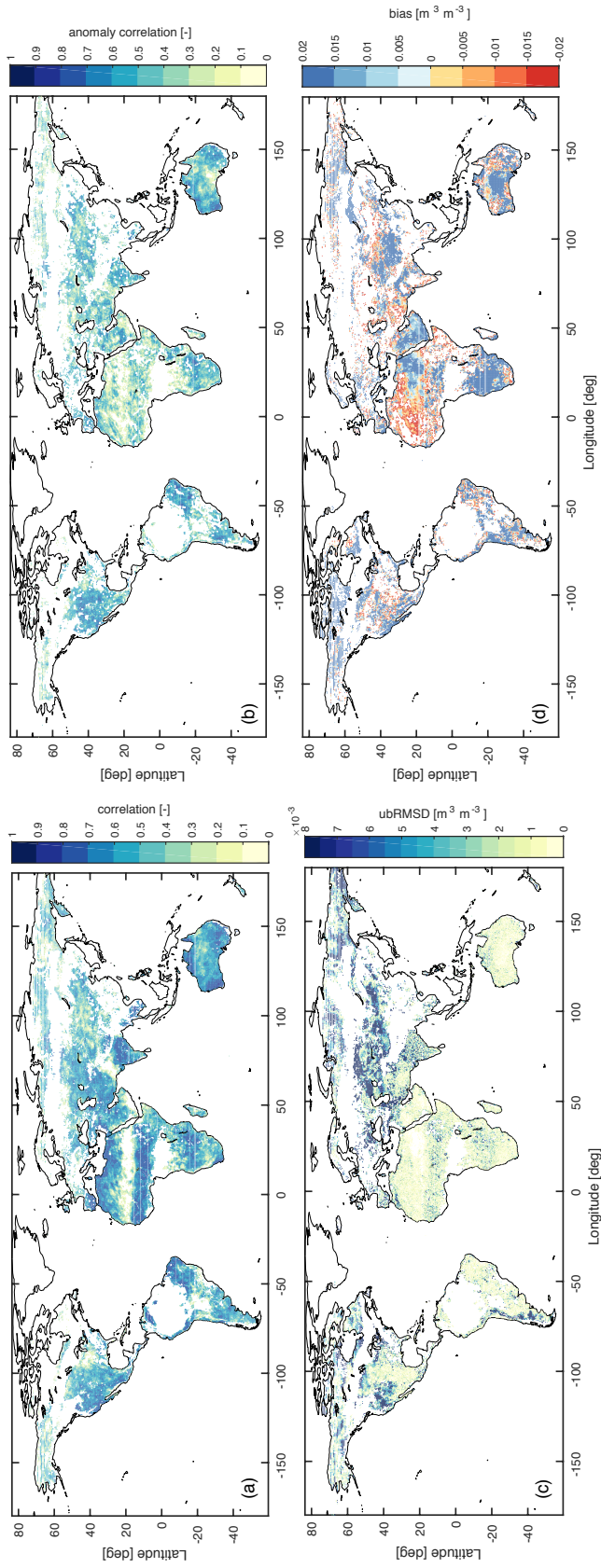


Figure 4: (a) Correlation, (b) anomaly correlation, (c) ubRMSD and (d) bias between the SMAP NN soil moisture retrievals and the GEOS-5 model soil moisture for data points from the evaluation period (April 2016 - March 2017). White spaces indicate areas with less than 30 data points, for which no robust metric could be computed.

498 The correlations (Figure 4 (a)) and anomaly correlations (Figure 4 (b)) ex-
499 hibit similar spatial patterns, with high values in the transition zones between
500 wet and dry climates and in regions with strong soil moisture variability, such as
501 the Sahel, Eastern Brazil and India. However, strong correlations and anomaly
502 correlations are also observed in semi-arid, sparsely to moderately vegetated
503 regions, such as the Western US, the Arabian Peninsula and large parts of Aus-
504 tralia. The (anomaly) correlations are lowest in arid regions (e.g., the Sahara
505 and Central Australia), where the soil moisture signal tends to be small and
506 noisy, as well as in extensive cropland regions (e.g., the US corn belt or the
507 croplands of Argentina, Uruguay and Paraguay), where irrigation and other
508 agricultural practices are likely to cause differences between the satellite re-
509 trieval product and the model.

510 The spatial patterns of the ubRMSD between the SMAP NN estimates and
511 the GEOS-5 soil moisture (Figure 4 (c)) are different from those observed for
512 the (anomaly) correlations, with large portions of the globe showing a ubRMSD
513 of less than $0.001 \text{ m}^3\text{m}^{-3}$, including Africa, Australia and large parts of South
514 America (excluding the Andes). Larger differences occur near mountainous
515 regions, such as the Rocky Mountains or the Southern Andes, likely caused
516 by higher uncertainty in the SMAP retrieval product. High-latitude boreal
517 regions, where the data availability is low and the model precipitation forcing
518 is less reliable (*Reichle and Liu, 2014*), also exhibit larger differences between
519 the NN retrieval product and the model. Finally, the ubRMSD between the NN
520 retrievals and the model estimates is large in the croplands of the US as well

521 as Southern Russia and Kazakhstan, which is possibly a result of the missing
522 representation of irrigation and other agricultural practices in the model that is
523 being corrected by the NN.

524 The bias between the NN estimates and the GEOS-5 model over the training
525 period (Figure 4 (d)) ranges between $-0.02 \text{ m}^3 \text{ m}^{-3}$ and $0.02 \text{ m}^3 \text{ m}^{-3}$ and, by
526 design, has a global average close to zero. In arid regions such as the Arabian
527 Peninsula, Central Australia or the Kalahari, the NN retrievals tend to indicate
528 wetter conditions than the GEOS-5 model. An exception is the Western Sahara,
529 where the NN retrievals show a dry bias with respect to the GEOS-5 estimates,
530 which might be an artifact of increased surface roughness in this region that
531 lowers the observed soil emissivity.

532 In order to illustrate the behavior of the NN retrievals relative to the GEOS-
533 5 model soil moisture in the training and evaluation periods, Figure 5 shows
534 the anomaly time series with respect to a 30-day moving average of the NN soil
535 moisture estimates (red squares) and the GEOS-5 model soil moisture (blue dia-
536 monds) for three SMAP core site stations - TxSON, Walnut Gulch and Carman.
537 (The figure also shows the in situ and L2P data, which will be discussed in sec-
538 tion 4.2.1). For better readability and to reduce the effect of seasonal differences,
539 we only plot the months April - September for 2015 and 2016 to represent the
540 training and evaluation periods, respectively, with the former indicated through
541 gray background shading. There is no obvious difference between the behavior
542 of the NN retrieval product in both periods, underlining once more the ability
543 of the trained NN to generalize beyond the training dataset. For the TxSON

544 (Figure 5 (a)) and Walnut Gulch (Figure 5 (b)) sites, the time series average
545 and dynamic range of the NN retrieval product and the GEOS-5 soil moisture
546 are comparable, but there are differences in the response to individual events,
547 illustrated for instance during the stronger drying in the NN soil moisture at
548 the TxSON station in June 2015. At the Carman site (Figure 5 (c)), the NN
549 soil moisture has a stronger variability compared to the model. This illustrates
550 that while the NN estimates globally match the bias and variability of the target
551 data, local biases and differences in variability between the NN estimates and
552 the target data occur.

553 *4.2. Evaluation against In Situ Observations*

554 In this section, we evaluate the skill of the NN retrieval product against
555 independent in situ soil moisture measurements from the SMAP core sites and
556 the ISMN (section 2.2.3). The skill of the NN retrievals is compared against
557 that of the GEOS-5 model soil moisture and the L2P retrievals. Only data from
558 the period April 2016 - March 2017 are used in the evaluation, since these data
559 did not contribute to the NN training.

560 *4.2.1. Core Site Data*

561 First, we assess the skill of the soil moisture products against core site in
562 situ measurements. The NN retrieval product has a higher correlation than the
563 GEOS-5 soil moisture for most core sites (Figure 6(a)), which is reflected in
564 the higher average correlation of 0.70 for the NN retrievals compared to 0.64
565 for the model. The model has higher correlations than both retrieval products

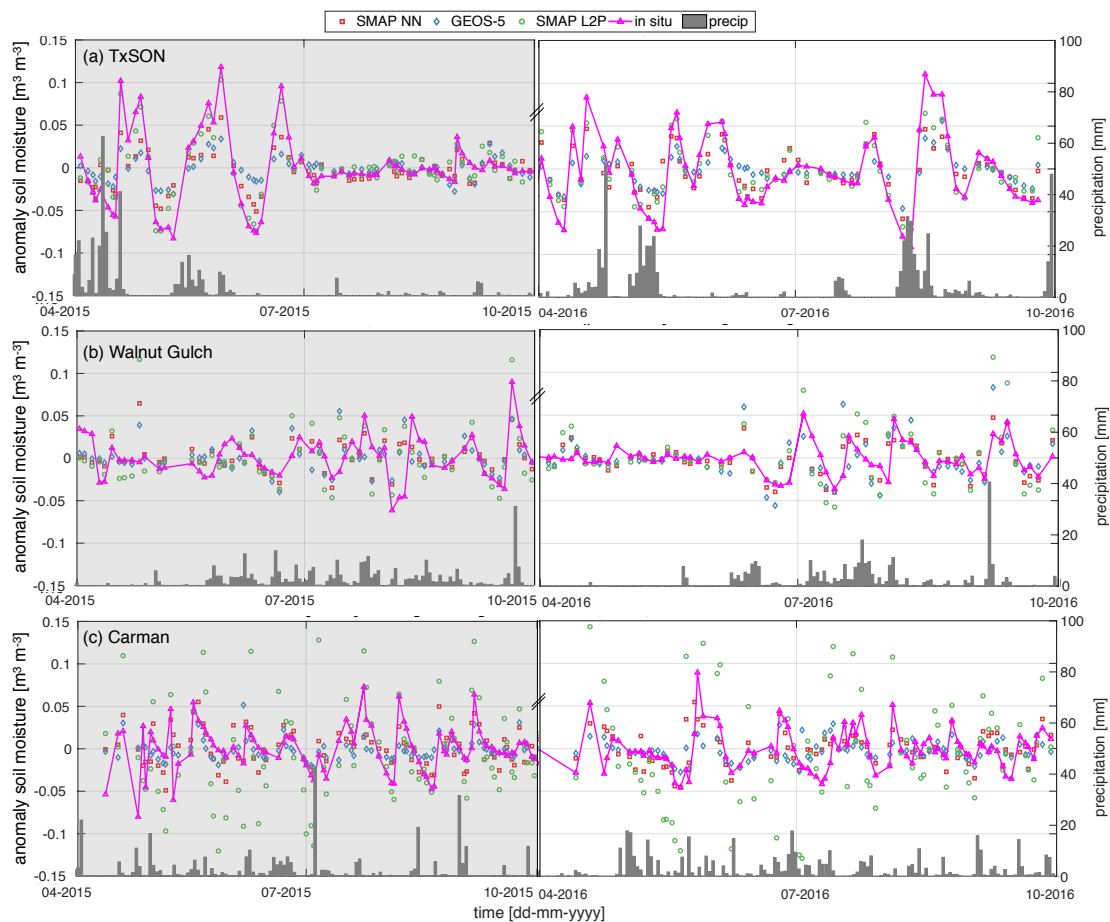


Figure 5: Soil moisture anomalies with respect to a 30-day moving average at the (a) TxSON, (b) Walnut Gulch and (c) Carman core sites for April - September of 2015 and 2016. Shown are the SMAP NN retrievals (red squares), the GEOS-5 model soil moisture (blue diamonds), the SMAP L2P retrievals (green circles) and the core site in situ soil moisture measurements (magenta triangles). Gray bars indicate the corrected GEOS-5 precipitation (section 2.1.2) interpolated to the ground station site. The gray background shading indicates data belonging to the training period.

566 at Reynolds Creek and a higher correlation than the NN retrievals at Carman
567 and Kenaston. The Carman and Kenaston watersheds are both located at
568 high latitudes where an incomplete seasonal cycle due to frozen soil filtering
569 could prevent the NN from accurately learning the SM-Tb relationship for such
570 conditions in the training phase. The NN retrievals tend to have a notably
571 higher skill than the model in moderately vegetated regions, such as the shrub-
572 and grassland sites of Little Washita or TxSON, as well as at most of the sites
573 characterized by an arid climate (see Table 1). However, while the results appear
574 to connect the relative performances of the NN product and model with climate
575 and land cover characteristics, more sites would be required to draw a firm
576 conclusion. The poor performance of the model at the South Fork site is partly
577 due to agricultural tile drainage, which is not accounted for in the model.

578 The L2P retrieval product has a higher correlation skill than both of the
579 other soil moisture products for the majority of core sites and consequently
580 has the highest average correlation of 0.78 (Figure 6(a)). The magnitude of
581 the skill difference between the two retrieval products is not obviously related
582 to the climate or land cover of the in situ sites. In regions with a moderate to
583 strong seasonal cycle, the correlation (R) primarily reflects the skill of capturing
584 seasonal soil moisture variations. Hence, the above results indicate a better
585 representation of the soil moisture seasonal cycle in the two retrieval products
586 compared to the model.

587 In terms of the anomaly correlations (Figure 6(b)), the NN retrieval product
588 has higher skill than the model estimates for most core sites and an average

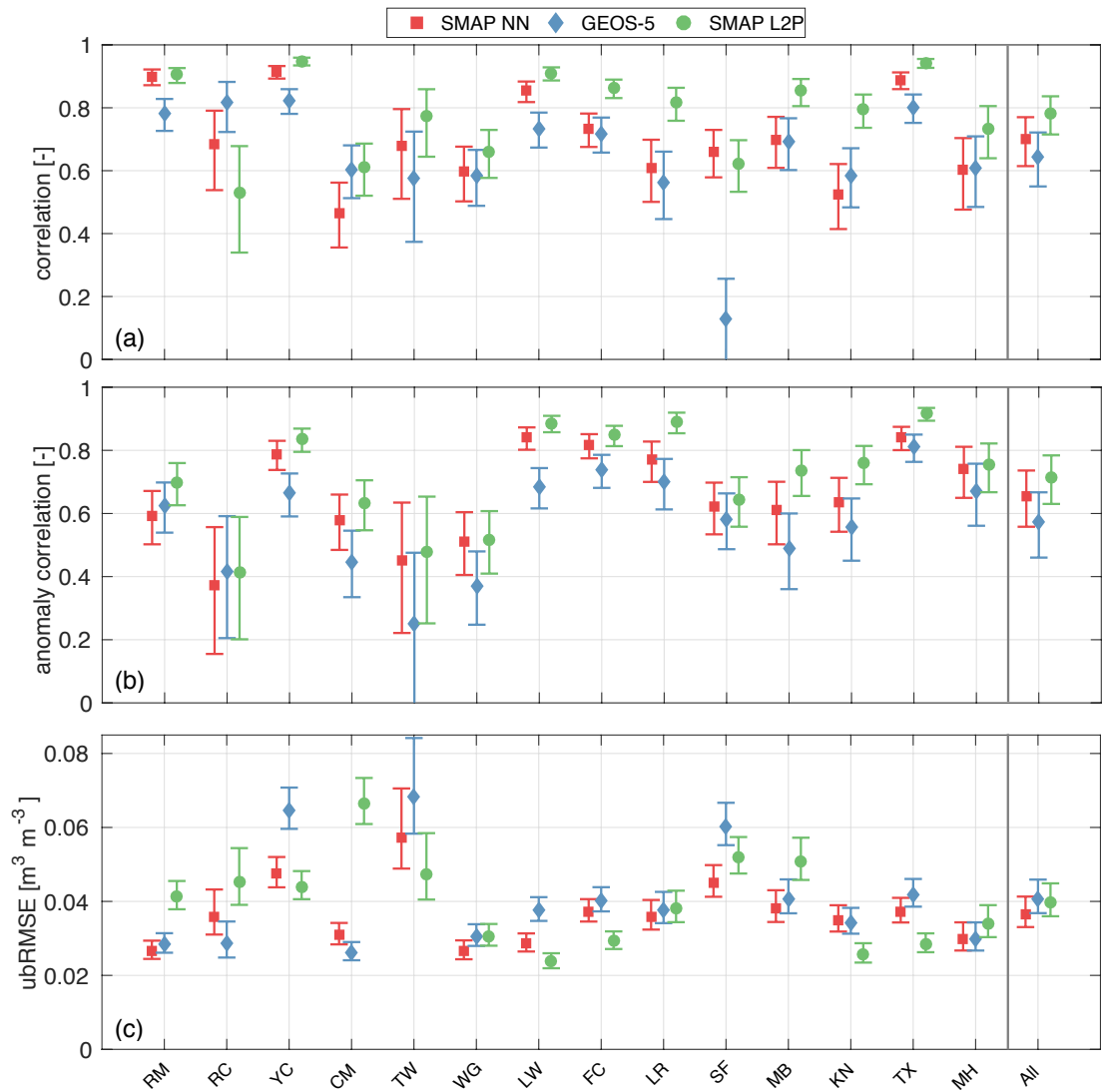


Figure 6: (a) Correlation, (b) anomaly correlation and (c) ubRMSE between the core site in situ measurements and the SMAP NN retrievals (red squares), the SMAP L2P retrievals (green circles) and the GEOS-5 model soil moisture (blue diamonds). Shown are the metrics for each site as well as the average across all sites. The error bars represent the 95% confidence interval.

589 skill of 0.66 compared to 0.57 for the model. The L2P retrieval product has the
590 highest average skill overall (0.71) as well as for a majority of the core sites.
591 In terms of the ubRMSE (Figure 6(c)), the skill of all three products is more
592 similar. The NN product has a somewhat lower error than the L2P product at
593 a majority of the stations and an overall lower average error of $0.037 \text{ m}^3\text{m}^{-3}$
594 compared to $0.041 \text{ m}^3\text{m}^{-3}$ for the L2P and GEOS-5 model estimates.

595 Our findings for the L2P skill are consistent (within error bars) with those
596 of *Colliander et al. (2017)* (not shown). The only significant difference occurs
597 at the Twente site, where *Colliander et al. (2017)* used a different set of sensors.
598 Compared to *Chan et al. (2016b)*, we obtain higher correlations and a slightly
599 larger ubRMSE for the L2P product. This is in part a result of the more
600 refined validation approach used by *Chan et al. (2016b)*, who generated special
601 L2P retrievals on custom grid cells that better match the locations of the in
602 situ measurements and thus did not perform the spatial interpolation that was
603 required for the published L2P retrievals used here (section 3.2). Other factors
604 contributing to the differences in the L2P metrics are the different validation
605 periods and L2P product versions used here and by *Chan et al. (2016b)*.

606 To further investigate the cause for the skill differences between the retrieval
607 products and the model at select sites, we now revisit Figure 5. At the TxSON
608 and Walnut Gulch sites the anomalies for both retrieval products follow the
609 in situ measurements very closely. The different average anomaly correlations
610 obtained for these sites are mostly due to different responses to isolated events.
611 An example is the dry down in June 2015 at the TxSON site, which is better

612 captured by the L2P retrievals than by the NN retrievals.

613 At the Carman site, both retrieval products are very noisy compared to the
614 model and in situ measurements (Figure 5(c)). The L2P product is noisier than
615 the NN product, which is also reflected in its higher ubRMSE at this site (see
616 Figure 6(c)). The higher ubRMSE might be caused by ancillary soil texture
617 data in the L2P retrieval algorithm that poorly describes the highly variable
618 conditions in the Carman watershed. This suggests that the NN retrieval ap-
619 proach has the potential to supplement the physically-based SMAP retrievals
620 in regions where the ancillary data used in the RTM are uncertain. Addition-
621 ally, both retrieval products suffer from using a VWC climatology that does not
622 accurately describe the rapidly changing vegetation dynamics at Carman.

623 The above results show that both SMAP retrieval products have higher cor-
624 relations than the model soil moisture with respect to the in situ measurements
625 (Figure 6). This is encouraging, given that most of the core sites are located in
626 North America, where models typically have been well tested and already have a
627 high skill (e.g. *Albergel et al. (2013)*). Additionally, the retrievals are at a slight
628 disadvantage in the comparison, since for most locations the SMAP emission
629 depth will be less than the 5 cm depth represented by the in situ measurements
630 and the model estimates. The better correlations of the retrieval products thus
631 illustrate the high quality of the SMAP observations and their potential to pro-
632 vide independent information that is not captured in the models, likely related
633 to agricultural practices, land use differences or phenology. This is corroborated
634 by the benefit of the SMAP brightness temperature assimilation performed in

635 the Level-4 soil moisture algorithm (*Reichle et al.*, 2017b (in press)).

636 Against the core site data, the L2P retrievals generally have a higher skill
637 than the NN retrievals in terms of the correlations and anomaly correlations,
638 while the NN retrievals have a better average ubRMSE (Figure 6). This behav-
639 ior could indicate the existence of a conditional bias in the SMAP NN retrievals,
640 as a result of dynamic range reduction that is typical for statistical techniques
641 (e.g. (*Kolassa et al.*, 2013)). The global average of the anomaly soil moisture
642 temporal standard deviations for the SMAP NN retrievals, the SMAP L2P re-
643 trievals and the GEOS-5 estimates are $0.020 \text{ m}^3 \text{ m}^{-3}$, $0.036 \text{ m}^3 \text{ m}^{-3}$ and 0.015
644 $\text{m}^3 \text{ m}^{-3}$, respectively, suggesting that the lower dynamic range of the NN re-
645 trievals compared to the L2P retrievals is driven by the lower dynamic range
646 of the model. At the core sites in Figure 5, the NN estimates appear to better
647 match to dynamic range of the in situ measurements than the L2P retrievals,
648 however, the limited number of core validation sites does not permit conclusions
649 regarding the general suitability of the retrieval products' dynamic range.

650 A notable exception from the typical relative skill ranking is the Reynolds
651 Creek site, where the NN retrievals have a significantly higher skill than the
652 L2P retrievals in terms of the correlations and ubRMSE. Since the retrieval
653 inputs are very similar for both products, the skill difference is likely caused by
654 uncertainties in the ancillary data used by the L2P algorithm (for example the
655 soil texture or roughness).

656 From the NN retrieval perspective, differences in the core site correlation skill
657 between the NN and L2P retrievals can be caused by (1) errors in the target

658 data, (2) errors in the satellite input data or (3) missing information in the NN
659 inputs. The first two error sources affect the quality of the NN fit, whereas
660 the latter would prevent the NN from capturing the full range of soil moisture
661 variability. Errors in the SMAP observations would affect both of the retrieval
662 products, such that target data errors or missing input information are more
663 likely causes for the slightly lower NN retrieval correlations against the core site
664 measurements. The results indicate that for the purpose of generating a 'stand-
665 alone' soil moisture retrieval product, the L2P retrieval algorithm is slightly
666 more suitable than the NN approach. However, our findings also demonstrated
667 the potential of the NN retrievals to supplement the physically-based approaches
668 in regions where the ancillary data or RTM parameterization is uncertain. The
669 core site results also show that the NN retrievals are of sufficient quality to
670 warrant further study into their assimilation as motivated above.

671 *4.2.2. International Soil Moisture Network*

672 Next, we analyze the NN retrieval skill against in situ measurements from the
673 ISMN. While these are single point measurements and thus less suitable than
674 the core site data for evaluating satellite retrievals, they are more numerous
675 and are available for a greater variety of climate and land cover conditions. As
676 before, we also estimate the skill of the L2P retrievals and the GEOS-5 model
677 estimates against the ISMN data for comparison.

678 In contrast to the evaluation against the core site data, the correlation skill
679 of the three soil moisture products against the ISMN measurements is more
680 similar, with an average correlation of 0.52 for the GEOS-5 model, 0.58 for the

681 NN retrievals and 0.56 for the L2P retrievals (Figure 7(a)). This suggests that
682 at the ISMN sites the NN retrievals slightly better capture the soil moisture
683 seasonal variations. However, the lower correlations compared to the core site
684 evaluation also illustrate that the single-sensor measurements of the ISMN less
685 adequately represent the retrieval and model spatial scales.

686 To further interpret the correlation differences between the three products,
687 Figure 8 maps the ranking of the three datasets, with the marker at each ISMN
688 site indicating the dataset with the highest skill. For better readability we only
689 plotted sites located in the contiguous US (i.e., iRON, PBO H2O, SCAN, SNO-
690 TEL, SOILSCAPE and USCRN), which constitutes the majority of sites used
691 in this study. A large part of the ISMN stations where a skill assessment was
692 possible are located in the Western US, as the screening for dense vegetation re-
693 duces the data availability in the Eastern US below the threshold for computing
694 a skill metric.

695 The model shows the highest correlation skill at many of the stations lo-
696 cated in or near the Rocky Mountains (Figure 8 (a)). In mountainous and
697 rough terrain the microwave retrievals are less reliable, because of the increased
698 surface roughness at the instrument footprint scale (*Schmugge et al.*, 1980).
699 Furthermore, the screening for frozen soil removes a large part of the SMAP
700 time series and reduces the retrieval algorithm’s ability to correctly capture
701 the soil moisture seasonal cycle in the training phase. In flatter regions away
702 from the mountains, such as the Central Valley, Arizona, South East New Mex-
703 ico or North Dakota, the retrievals mostly have higher correlations than the

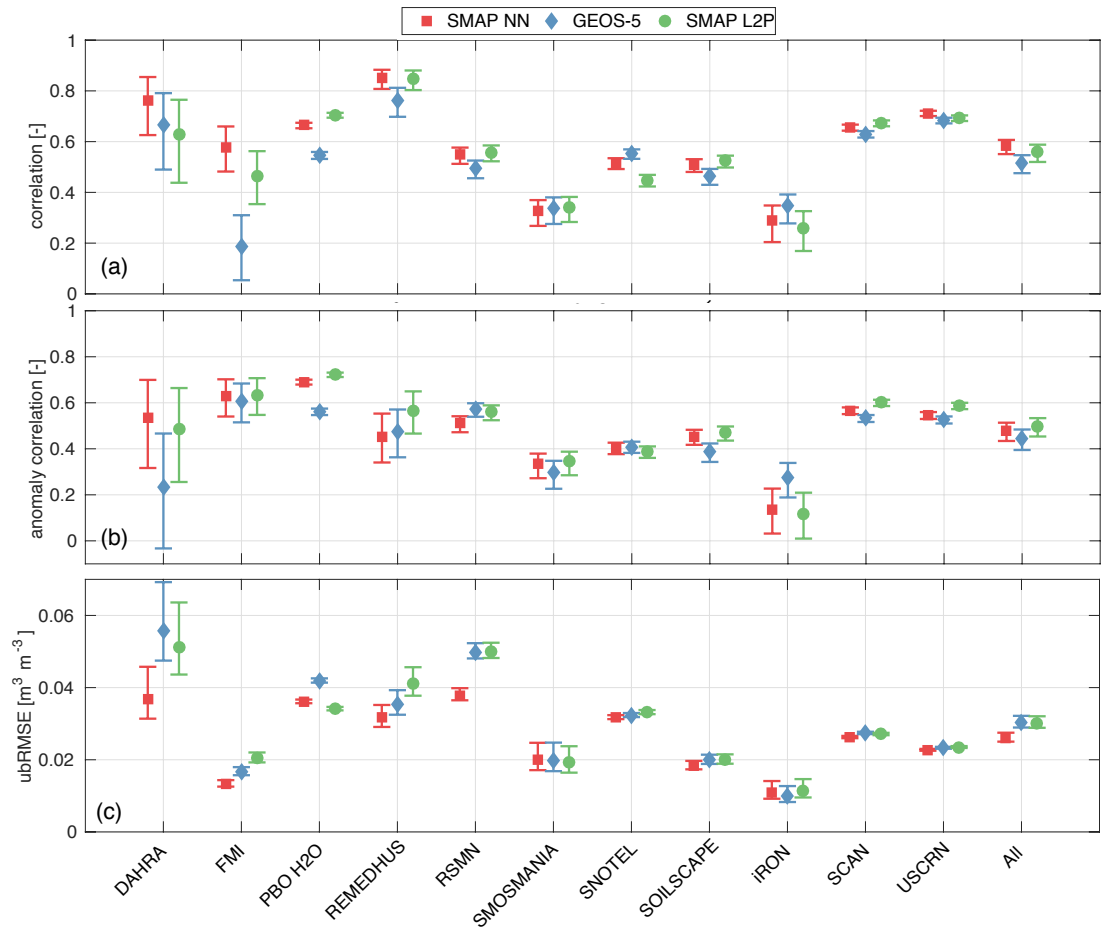


Figure 7: Network average (a) correlation, (b) anomaly correlation and (c) ubRMSE between the ISMN in situ observations and the SMAP NN retrievals (red squares), the SMAP L2P retrievals (green circles) and the GEOS-5 model soil moisture (blue diamonds). Shown are the metrics for each network as well as the average across all networks. All averages are cluster-based (section 3.2) The error bars represent the 95% confidence interval.

704 model (Figure 8 (a)). Thus, the high station density near the Rocky Mountains
705 slightly skews the average correlation in favor of the model resulting in a model
706 correlation that is comparable to those of the retrieval products. Our clustering
707 approach (section 3.2) mitigates this skew to some extent, but with a cluster
708 spatial extent limited to 1° , we still use a higher number of clusters in the Rocky
709 Mountain region than in other parts of the US. A longer SMAP time series will
710 allow for more correlations to be computed for stations in the Eastern US and
711 would likely lead to different relative correlation skill values for the retrievals
712 and the model estimates.

713 It is worth noting that our correlation value of 0.65 versus SCAN for the
714 SMAP NN retrievals (Figure 7 (a)) is similar to the 0.61 correlation versus
715 SCAN obtained for SMOS NN retrievals by *Rodriguez-Fernández et al.* (2015).
716 However, it is not possible to draw firm conclusions regarding the relative quality
717 of the SMAP and SMOS NN products, owing to the differences in the validation
718 period and data quality control between *Rodriguez-Fernández et al.* (2015) and
719 our study.

720 In terms of the network average anomaly correlations (Figure 7(b)), the
721 L2P retrievals have the highest skill with an average anomaly correlation of
722 0.50 compared to 0.48 and 0.44 for the NN and GEOS-5 products, respectively.
723 Investigating the ranking in terms of the anomaly correlations (Figure 8(b))
724 shows that the L2P product has the highest anomaly correlation for most of the
725 stations leading to the highest average anomaly correlation.

726 Finally, the NN retrievals have the lowest average ubRMSE of 0.026 m^3

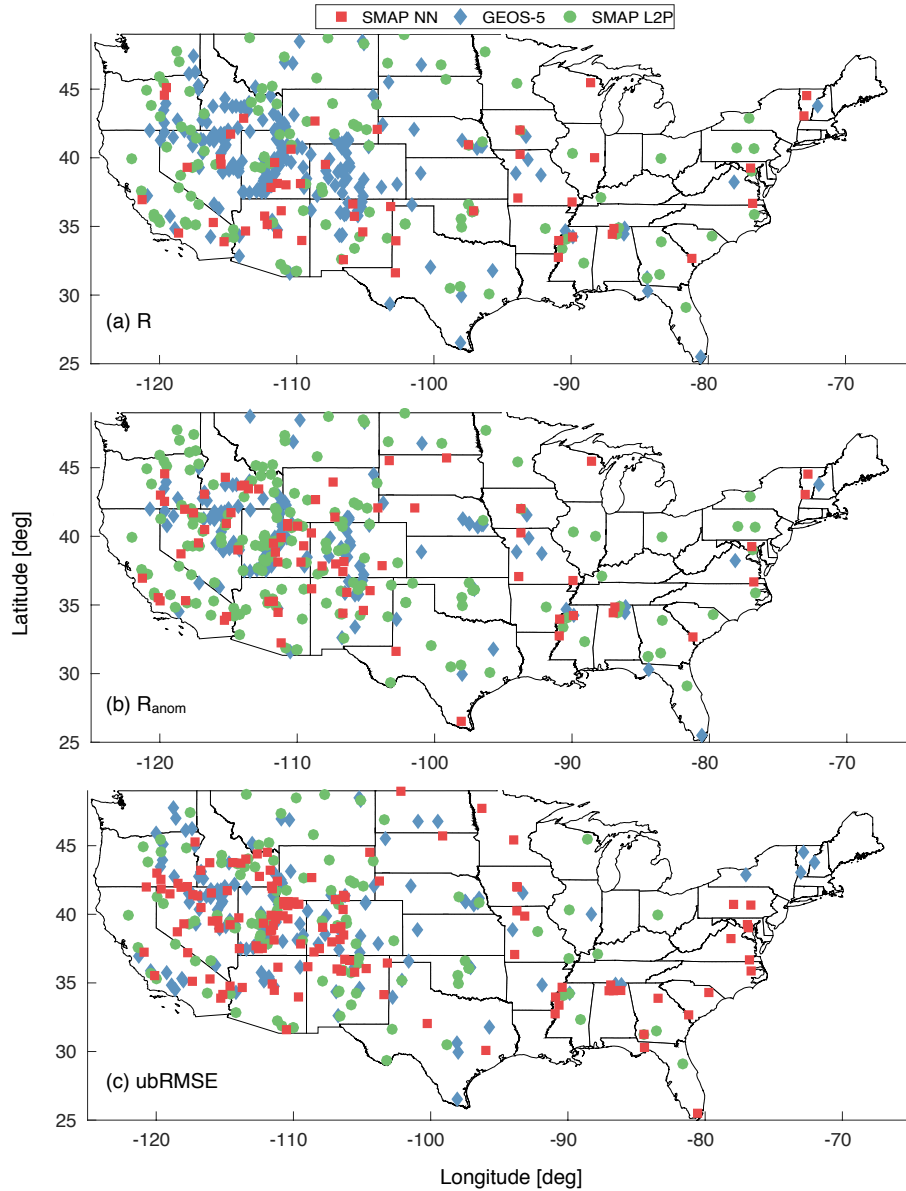


Figure 8: Skill ranking in terms of (a) correlation, (b) anomaly correlation and (c) ubRMSE of the SMAP NN retrievals (red squares), the GEOS-5 model soil moisture (blue diamonds) and the SMAP L2P retrievals (green circles) at the ISMN stations located in the US. Each marker indicates the dataset that obtained the highest skill at a given station. The contributing networks are iRON, PBO H2O, SCAN, SNOTEL, SOILSCAPE and USCRN.

727 m^{-3} compared to $0.030 \text{ m}^3 \text{ m}^{-3}$ for the L2P retrievals and the GEOS-5 esti-
728 mates (Figure 7(c)). This relative behavior is largely driven by a significantly
729 lower ubRMSE for the NN retrievals against the DAHRA and RSMN networks.
730 Across all stations, the ubRMSE ranking of the three products in Figure 8(c)
731 is fairly evenly distributed. This also indicates that the lower network average
732 errors observed for the L2P product are not consistent, but driven by a few
733 stations with a low L2P error.

734 Overall, the correlations of all three products with respect to the ISMN data
735 are lower than for the comparison against the core site data, owing to the lower
736 representativeness of the ISMN stations compared to the core sites.

737 *4.3. Triple Collocation Analysis*

738 For a global evaluation of the SMAP retrieval products and the GEOS-5
739 model estimates, we estimate the fractional error standard deviations using the
740 TC analysis (section 3.3).

741 The fractional error spatial patterns mostly show good agreement across the
742 three soil moisture products (Figure 9), corroborated by the very similar global
743 mean fractional error of ~ 1.1 for all three products. All products have fractional
744 errors higher than 1 in the arid and semi-arid regions of the Sahara, the Tibetan
745 Plateau, Northern Mexico and the Northern Arabian Peninsula, indicating that
746 the noise (even though it is small in absolute terms) dominates the small soil
747 moisture signal here and limits the accuracy of all three products. Other arid
748 and semi-arid regions, however, including most of Australia, Southwest Africa
749 and the Southern Andes, have low fractional errors for all products. This in-

750 dicates that the local fractional errors are driven by a combination of factors,
751 likely including the mean soil moisture level, the surface roughness, land cover
752 and soil type.

753 Despite a general similarity of the fractional error spatial patterns of all three
754 soil moisture products, several differences between the retrieval and model error
755 patterns exist. For example, the GEOS-5 estimates have higher errors than
756 the retrieval products in the high latitude boreal regions of Alaska and Eastern
757 Siberia, where the precipitation forcing is less reliable (*Reichle and Liu, 2014*).
758 In contrast, both retrieval products have higher fractional errors than the model
759 in areas surrounding the tropical forests, where a denser vegetation cover limits
760 the canopy penetration of the microwave signal and the higher surface roughness
761 increases the signal noise.

762 The NN and L2P retrieval products show a generally good agreement of
763 the fractional error spatial patterns, but differences in the absolute values exist
764 (Figure 10). For example, the L2P retrievals tend to have lower fractional errors
765 (or noise-to-signal ratios) in the arid regions of Central Australia, the Kalahari
766 or the Southern Sahara, possibly indicating that the ancillary soil data used by
767 the L2P algorithm allows it to better account for the effect of surface roughness,
768 which can be significant in arid regions. However, this behavior is not observed
769 in other arid areas, such as the Central Sahara or the Arabian Peninsula. The
770 NN retrievals have a lower fractional error in moderately to densely vegetated
771 regions and transition zones, such as India, Central Africa, Eastern Brazil and
772 Northern Australia. This suggests that in these regions, the NN method can

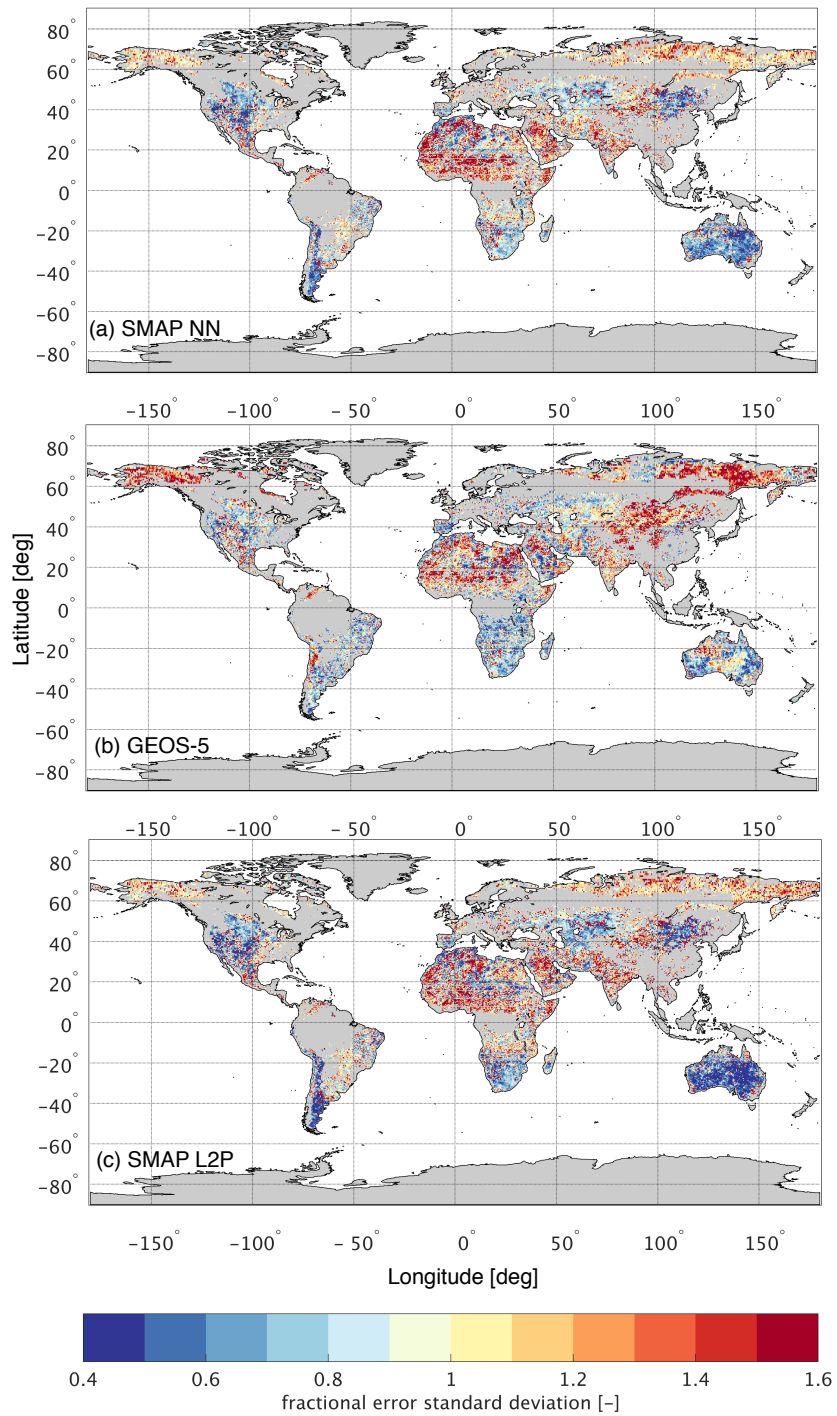


Figure 9: Fractional error standard deviations estimated from TC for the (a) SMAP NN retrieval product, (b) GEOS-5 modeled soil moisture and (c) SMAP L2P retrieval product.

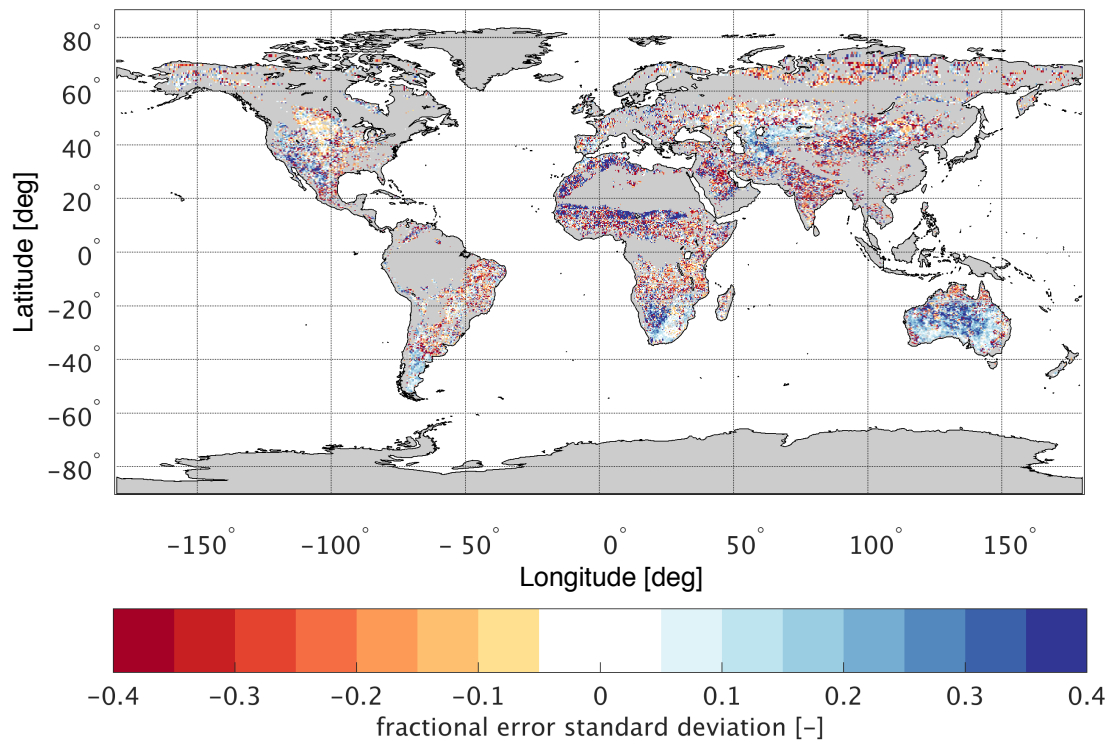


Figure 10: Difference of the fractional error standard deviations between the NN and L2P retrievals (NN - L2P). Negative values (red) indicate a lower fractional error and higher signal-to-noise ratio for the NN retrievals and positive values (blue) indicate a lower fractional error of the L2P retrievals.

773 produce soil moisture estimates with a higher certainty and could be used to
774 supplement or improve the L2P retrievals. However, due to the lack of in situ
775 stations in these areas, this finding cannot be further corroborated.

776 While the characterization of the global error distributions is informative,
777 it is important to keep in mind that the error estimates derived from the TC
778 analysis here are also subject to uncertainties. These are related to (1) differ-
779 ences in the overpass times between AMSR2 and ASCAT relative to SMAP and
780 the simulation times of the model, (2) the slightly lower emission depth of the
781 higher frequency AMSR2 and ASCAT data compared to SMAP and the depth
782 of the model’s surface layer, and (3) potential errors in the porosity data used
783 to convert the ASCAT data into volumetric surface soil moisture estimates.

784 **5. Summary**

785 In this study we developed and evaluated a NN based retrieval algorithm
786 to estimate global surface soil moisture from SMAP brightness temperatures.
787 The SMAP NN retrieval product was trained on GEOS-5 model estimates and
788 evaluated against in situ measurements from the SMAP core validation sites
789 and the ISMN. The skill of the NN retrieval was compared against that of the
790 GEOS-5 estimates and the SMAP L2P retrievals.

791 The comparison of the SMAP NN retrieval product against the GEOS-5
792 model soil moisture showed that globally the two datasets agree well. Differ-
793 ences occur in mountainous regions, where the microwave satellite retrievals are
794 uncertain, and in agricultural areas, where the satellite retrieval product possi-

795 bly captures the result of agricultural practices (such as irrigation, tilling and
796 harvesting) that are not represented in the model. Combined with the generally
797 higher skill of the SMAP retrievals against in situ measurements, the results con-
798 firm the potential for the SMAP observations to inform a model through data
799 assimilation, as has been shown with the SMAP Level-4 products (*Reichle et*
800 *al.*, 2017b (in press)).

801 The SMAP NN soil moisture estimates compare favorably against the SMAP
802 core site in situ measurements with an average correlation and anomaly corre-
803 lation of 0.70 and 0.66, respectively, and an average ubRMSE of $0.037 \text{ m}^3\text{m}^{-3}$.
804 Evaluated against ISMN sparse network in situ measurements, the correlation
805 and anomaly correlation were 0.58 and 0.48, respectively, and the ubRMSE was
806 $0.026 \text{ m}^3\text{m}^{-3}$. The core site data better represent the spatial scales of a satel-
807 lite footprint or model grid cell, leading to the higher skill of the NN retrieval
808 against core site data than against ISMN data.

809 The NN retrievals had a higher correlation (by 0.06) and a higher anomaly
810 correlation (by 0.09) against core site in situ measurements than the GEOS-5
811 model estimates, which were used as the NN target data. The corresponding
812 average ubRMSE of the NN retrievals was $0.004 \text{ m}^3\text{m}^{-3}$ lower than that of the
813 GEOS-5 estimates. Evaluated against ISMN data, the relative skill of the NN
814 retrievals and model estimates was comparable to that found during the core
815 site evaluation.

816 Overall, the results suggest that (1) the NN retrievals are able to use the
817 SMAP brightness temperatures to correct potential errors in the model-based

818 target data and (2) the NN retrievals capture soil moisture information not
819 present in the model, resulting in better agreement with the core site and ISMN
820 in situ measurements. The latter indicates that the NN retrievals may be benefi-
821 cial in data assimilation, in particular for the short-term soil moisture variations
822 (captured by the anomaly correlations against the cores sites) for which the skill
823 difference between the retrievals and the model estimates is highest.

824 Generally, the (anomaly) correlation skill of the NN retrievals against core
825 site measurements is lower than that of the SMAP L2P product (by 0.08 and
826 0.05 for the correlations and anomaly correlations, respectively). The ubRMSE
827 of the NN retrievals, however, is lower than that of the L2P retrievals by 0.004
828 m^3m^{-3} . Evaluated against ISMN data, which represent a more diverse set
829 of local conditions but only provide point-scale information, the NN and L2P
830 retrievals have a very similar (anomaly) correlation skill, but the NN retrievals
831 have a lower ubRMSE (by 0.04 m^3m^{-3}) than the L2P retrievals. The slightly
832 lower (anomaly) correlation skill of the NN retrievals at the core sites is most
833 likely related to errors in the training target data or missing information in the
834 input data, whereas the higher ubRMSE of the L2P retrieval at the core sites
835 is likely related to the higher time series variability of this product.

836 A triple collocation analysis using AMSR2 and ASCAT soil moisture re-
837 trievals as the additional two datasets showed that at the global scale all three
838 products have comparable errors relative to their respective soil moisture dy-
839 namic range. The NN and L2P retrieval products have very similar error spa-
840 tial patterns, but the NN retrievals have a better skill than the L2P product in

841 densely vegetated regions and transition zones outside of CONUS. The GEOS-5
842 model has a slightly different error spatial patterns compared to the retrievals,
843 with notable differences in high latitudes, where the model has higher errors
844 owing to the increased uncertainty in its precipitation forcing, and in densely
845 vegetated areas, where the retrieval products are less reliable owing to the lower
846 soil moisture sensitivity of SMAP brightness temperatures in the presence of
847 dense vegetation.

848 Overall, the skill of the SMAP NN retrievals is only slightly worse than that of the
849 SMAP L2P retrieval product, but the NN retrievals are provided in the global
850 climatology of the GEOS-5 model, which may reduce the need for further bias
851 correction before data assimilation. Local biases between the NN retrievals and
852 the model, however, are retained in the NN retrievals, which would violate typ-
853 ical data assimilation requirements. Additionally, local discrepancies between
854 the dynamic range of the NN retrievals and the model estimates could result in
855 non-orthogonal errors between the observations and the model estimates, which
856 would also violate typical data assimilation requirements. Consequently, fur-
857 ther investigation is needed to determine the impact of such violations on the
858 quality of the hydrological fields and surface flux estimates obtained from data
859 assimilation, and whether the assimilation system can use NN retrievals more
860 efficiently than standard retrievals or brightness temperatures.

861 The natural next step is thus to assimilate the SMAP NN retrieval product
862 and compare the resulting analysis skill against that of assimilation experiments
863 using traditional localized or other non-localized bias correction techniques, and

864 against the assimilation of L2P retrievals and brightness temperatures. Another
865 possible extension to this study would be to use the higher-resolution SMAP
866 Enhanced Level-1C brightness temperature product (*Chaubell et al.*, 2016) to
867 generate SMAP NN soil moisture retrievals at a higher spatial resolution.

868 **Acknowledgments**

869 J. Kolassa was supported by the NASA Postdoctoral Program, adminis-
870 tered by Universities Space Research Association under contract with NASA.
871 Additional funding was provided by the NASA Soil Moisture Active Passive
872 mission. P. Gentine was supported by grant NNX15AB30G. Computational re-
873 sources for this study were provided by the NASA High-End Computing (HEC)
874 Program through the NASA Center for Climate Simulation (NCCS) at the God-
875 dard Space Flight Center. We thank Aaron Berg, Tracy Rowlandson and Erica
876 Tetlock for providing soil moisture measurements from the Kenaston network,
877 which is funded by Environment and Climate Change Canada and the Cana-
878 dian Space Agency. We also thank Mark Seyfried and Rogier van der Velde
879 for providing soil moisture measurements from the Reynolds Creek and Twente
880 networks, respectively.

881 **References**

882 Aires, F., Prigent, C., and Rossow, W.B. (2005), Sensitivity of satel-
883 lite microwave and infrared observations to soil moisture at a global

884 scale: 2. Global statistical relationships, *J. Geophys. Res.*, *110*, D11103,
885 doi:10.1029/2004JD005094.

886 Albergel, C., Dorigo, W., Reichle, R.H., Balsamo, G., De Rosnay, P., Muoz-
887 Sabater, J., Isaksen, L., De Jeu, R. and Wagner, W., (2013). Skill and global
888 trend analysis of soil moisture from reanalyses and microwave remote sensing.
889 *Journal of Hydrometeorology*, *14*(4), pp.1259-1277. doi:10.1175/JHM-D-12-
890 0161.1 Vancouver

891 Al Bitar, A., Leroux, D., Kerr, Y.H., Merlin, O., Richaume, P., Sa-
892 hoo, A. and Wood, E.F., (2012). Evaluation of SMOS soil moisture
893 products over continental US using the SCAN/SNOTEL network. *IEEE*
894 *Transactions on Geoscience and Remote Sensing*, *50*(5), pp.1572-1586.
895 doi:10.1109/TGRS.2012.2186581

896 Alemohammad, S.H., Fang, B., Konings, A.G., Green, J.K., Kolassa, J., Pri-
897 gent, C., Aires, F., Miralles, D. and Gentile, P., (2017) Water, Energy, and
898 Carbon with Artificial Neural Networks (WECANN): A statistically-based
899 estimate of global surface turbulent fluxes using solar-induced fluorescence.
900 *Biogeosciences Discussions*. doi:10.5194/bg-2016-495

901 Assouline, S. (2013), Infiltration into soils: Conceptual approaches and solu-
902 tions, *Water Resources Research* *49*(4), 1755-1772. doi:10.1002/wrcr.20155

903 Bateni, S. M., and Entekhabi, D. (2012). Relative efficiency of land
904 surface energy balance components. *Water Resources Research*,
905 *48*(4).doi:10.1029/2011WR011357

906 Bartalis, Z., Naeimi, V., Hasenauer, S. and Wagner, W., (2008). ASCAT soil
907 moisture product handbook. *ASCAT Soil Moisture Report Series*, 15.

908 Belward, A.S., Estes, J.E. and Kline, K.D., (1999). The IGBP-DIS global 1-km
909 land-cover data set DISCover: A project overview. *Photogrammetric Engi-*
910 *neering and Remote Sensing*, 65(9), pp.1013-1020.

911 Brodzik, M.J., Billingsley, B., Haran, T., Raup, B. and Savoie, M.H., (2012).
912 EASE-grid 2.0: incremental but significant improvements for Earth-gridded
913 data sets. *ISPRS International Journal of Geo-Information*, 1(1), pp.32-45.
914 doi:10.3390/ijgi1010032

915 Calvet, J.C., Fritz, N., Froissard, F., Suquia, D., Petitpa, A. and Piguët, B.,
916 (2007), July. In situ soil moisture observations for the CAL/VAL of SMOS:
917 the SMOSMANIA network. *Geoscience and Remote Sensing Symposium*,
918 2007. IGARSS 2007. IEEE International (pp. 1196-1199). IEEE.

919 Chai, S.S., Walker, J.P., Makarynskyy, O., Kuhn, M., Veenendaal, B. and West,
920 G., (2009). Use of soil moisture variability in artificial neural network retrieval
921 of soil moisture. *Remote Sensing*, 2(1), pp.166-190. doi:10.3390/rs2010166

922 Chan, S., E. G. Njoku, and A. Colliander. (2016). SMAP L1C Radiometer
923 Half-Orbit 36 km EASE-Grid Brightness Temperatures, Version 3. Boulder,
924 Colorado USA. *NASA National Snow and Ice Data Center Distributed Active*
925 *Archive Center*. doi: <http://dx.doi.org/10.5067/E51BSP6V3KP7>.

926 Chan, S.K., Bindlish, R., O'Neill, P.E., Njoku, E., Jackson, T., Collian-
927 der, A., Chen, F., Burgin, M., Dunbar, S., Piepmeier, J. and Yueh, S.,

928 (2016b). Assessment of the SMAP passive soil moisture product. *IEEE*
929 *Transactions on Geoscience and Remote Sensing*, 54(8), pp.4994-5007.
930 doi:10.1109/TGRS.2016.2561938

931 Chaubell, M. J., S. Chan, R. S. Dunbar, J. Peng, and S. Yueh. (2016). SMAP
932 Enhanced L1C Radiometer Half-Orbit 9 km EASE-Grid Brightness Tempera-
933 tures, Version 1. Boulder, Colorado USA. NASA National Snow and Ice Data
934 Center Distributed Active Archive Center. doi:10.5067/2C9O9KT6JAWS.

935 Chen, F., Crow, W.T., Colliander, A., Cosh, M.H., Jackson, T.J., Bindlish,
936 R., Reichle, R.H., Chan, S.K., Bosch, D.D., Starks, P.J. and Goodrich,
937 D.C., (2016). Application of triple collocation in ground-based validation
938 of Soil Moisture Active/Passive (SMAP) level 2 data products. *IEEE Jour-*
939 *nal of Selected Topics in Applied Earth Observations and Remote Sensing*.
940 doi:10.1109/JSTARS.2016.2569998

941 Colliander, A., Jackson, T.J., Bindlish, R., Chan, S., Das, N., Kim, S.B., Cosh,
942 M.H., Dunbar, R.S., Dang, L., Pashaian, L. and Asanuma, J., (2017). Val-
943 idation of SMAP surface soil moisture products with core validation sites.
944 *Remote Sensing of Environment*, 191, pp.215-231.

945 Corradini, C., Morbidelli, R., and Melone, F. (1998). On the interaction be-
946 tween infiltration and Hortonian runoff. *Journal of Hydrology*, 204(1), 52-67.
947 doi:10.1016/S0022-1694(97)00100-5

948 Cybenko, G.V. (1989), Approximation by superpositions of a sigmoidal

949 function, *Mathematics of Control, Signals and Systems*, 2, 303–314. doi:
950 10.1007/BF02551274

951 De Lannoy, G. J., Koster, R. D., Reichle, R. H., Mahanama, S. P., and Liu,
952 Q. (2014). An updated treatment of soil texture and associated hydraulic
953 properties in a global land modeling system. *Journal of Advances in Modeling
954 Earth Systems*, 6(4), 957-979. doi: 10.1002/2014MS000330

955 De Lannoy, G. J. M., R. H. Reichle, J. Peng, Y. Kerr, R. Castro, E. J. Kim,
956 and Q. Liu (2015), Converting Between SMOS and SMAP Level-1 Bright-
957 ness Temperature Observations Over Nonfrozen Land, *IEEE Geoscience and
958 Remote Sensing Letters*, 12, 1908-1912, doi:10.1109/LGRS.2015.2437612.

959 De Lannoy, G.J. and Reichle, R.H., (2016). Global assimilation of multiangle
960 and multipolarization SMOS brightness temperature observations into the
961 GEOS-5 catchment land surface model for soil moisture estimation. *Journal
962 of Hydrometeorology*, 17(2), pp.669-691. doi:10.1175/JHM-D-15-0037.1

963 Diamond, H.J., Karl, T.R., Palecki, M.A., Baker, C.B., Bell, J.E., Leeper, R.D.,
964 Easterling, D.R., Lawrimore, J.H., Meyers, T.P., Helfert, M.R. and Goadge,
965 G., (2013). US Climate Reference Network after one decade of operations:
966 Status and assessment. *Bulletin of the American Meteorological Society*, 94(4),
967 pp.485-498. doi:10.1175/BAMS-D-12-00170.1

968 Dorigo, W. A., Wagner, W., Hohensinn, R., Hahn, S., Paulik, C., Xaver, A.,
969 Gruber, A., Drusch, M., Mecklenburg, S., van Oevelen, P., Robock, A., and
970 Jackson, T. (2011). The International Soil Moisture Network: a data hosting

971 facility for global in situ soil moisture measurements, *Hydrology and Earth*
972 *System Science*, 15, 1675-1698. doi:10.5194/hess-15-1675-2011

973 Draper, C.S., Reichle, R., de Jeu, R., Naeimi, V., Parinussa, R. and Wagner, W.,
974 (2013). Estimating root mean square errors in remotely sensed soil moisture
975 over continental scale domains. *Remote Sensing of Environment*, 137, pp.288-
976 298. doi:10.1016/j.rse.2013.06.013

977 Ducharne, A., Koster, R.D., Suarez, M.J., Stieglitz, M. and Kumar, P., (2000).
978 A catchment-based approach to modeling land surface processes in a general
979 circulation model: 2. Parameter estimation and model demonstration. *Journal*
980 *of Geophysical Research*, 105(24), pp.823-24. doi:10.1029/2000JD900328

981 Entekhabi, D., Nakamura, H. and Njoku, E.G., (1994). Solving the inverse
982 problem for soil moisture and temperature profiles by sequential assimila-
983 tion of multifrequency remotely sensed observations. *IEEE Transactions on*
984 *Geoscience and Remote Sensing*, 32(2), pp.438-448. doi:10.1109/36.295058

985 Entekhabi, D., Njoku, E. G., O'Neill, P. E., Kellogg, K. H., Crow, W. T.,
986 Edelstein, W. N. (2010), The Soil Moisture Active Passive (SMAP) Mission,
987 *Proceedings of the IEEE* 98(5), 704–716. doi:10.1109/JPROC.2010.2043918.

988 Figa-Saldaña, J., Wilson, J. J., Attema, E., Gelsthorpe, R., Drinkwater, M.
989 R., and Stoffelen, A. (2002). The advanced scatterometer (ASCAT) on the
990 meteorological operational (MetOp) platform: A follow on for European
991 wind scatterometers. *Canadian Journal of Remote Sensing*, 28(3), 404-412.
992 doi:10.5589/m02-035

993 World Meteorological Organization - Global Climate Observing System (2009).
994 Guideline for the Generation of Satellite-based Datasets and Products
995 meeting GCOS Requirements. *WMO Technical Document* 1488 [https://public.wmo.int/en/programmes/global-climate-observing-system/
996 //public.wmo.int/en/programmes/global-climate-observing-system/
997 Publications/gcos-143.pdf](https://public.wmo.int/en/programmes/global-climate-observing-system/Publications/gcos-143.pdf)

998 Gentine, P., Polcher, J., and Entekhabi, D. (2011). Harmonic prop-
999 agation of variability in surface energy balance within a coupled
1000 soil-vegetation-atmosphere system. *Water Resources Research*, 47(5).
1001 doi:10.1029/2010WR009268

1002 Gruber, A., Su, C.H., Zwieback, S., Crow, W., Dorigo, W. and Wagner, W.,
1003 (2016). Recent advances in (soil moisture) triple collocation analysis. *Interna-
1004 tional Journal of Applied Earth Observation and Geoinformation*, 45, pp.200-
1005 211. doi:10.1016/j.jag.2015.09.002

1006 Jackson, T.J., Colliander, A., Kimball, J., Reichle, R., Derksen, C., Crow,
1007 W., Entekhabi, D., O'Neill, P. and Njoku, E., 2014. SMAP Science Data
1008 Calibration and Validation Plan (Revision A), *Soil Moisture Active Passive
1009 (SMAP) Mission Science Document. JPL D-52544*. Jet Propulsion Labo-
1010 ratory, Pasadena, CA. [https://smap.jpl.nasa.gov/files/smap2/CalVal_
1011 Plan_120706_pub.pdf](https://smap.jpl.nasa.gov/files/smap2/CalVal_Plan_120706_pub.pdf)

1012 Jackson, T.J., P. O'Neill, E. Njoku, S, Chan, R. Bindlish, A. Colliander,
1013 F. Chen, M. Burgin, S. Dunbar, J. Piepmeier, M. Cosh, T. Caldwell, J.
1014 Walker, X. Wu, A. Berg, T. Rowlandson, A. Pacheco, H. McNairn, M.

1015 Thibeault, J. Martnez-Fernndez, . Gonzlez-Zamora, M. Seyfried, D. Bosch,
1016 P. Starks, D. Goodrich, J. Prueger, Z. Su, R. van der Velde, J. Asanuma,
1017 M. Palecki, E. Small, M. Zreda, J. Calvet, W. Crow, Y. Kerr, S. Yueh,
1018 and D. Entekhabi (2016). Calibration and Validation for the L23_SM_P Ver-
1019 sion 3 Data Products, *SMAP Project, JPL D-93720*, Jet Propulsion Lab-
1020 oratory, Pasadena, CA. http://nsidc.org/data/docs/daac/smap/sp_12_smp/pdfs/L2SMP_validated_assess_rpt_rel2_v10a_final.pdf
1021

1022 Jimenez, C., Clark, D. B., Kolassa, J., Aires, F., and Prigent, C. (2013). A joint
1023 analysis of modeled soil moisture fields and satellite observations. *J. Geophys.*
1024 *Res*, 118(12), 6771-6782. doi: 10.1002/jgrd.50430

1025 Jung, M., Reichstein, M., Schwalm, C.R., Huntingford, C., Sitch, S., Ahlström,
1026 A., Arneth, A., Camps-Valls, G., Ciais, P., Friedlingstein, P. and Gans, F.,
1027 (2017). Compensatory water effects link yearly global land CO2 sink changes
1028 to temperature. *Nature*, 541(7638), pp.516-520. doi:10.1038/nature20780

1029 Kasahara, M., Imaoka, K., Kachi, M., Fujii, H., Naoki, K., Maeda, T.,
1030 Ito, N., Nakagawa, K. and Oki, T., (2012), Status of AMSR2 on GCOM-
1031 W1. *SPIE Remote Sensing* (pp. 853307-853307). International Society
1032 for Optics and Photonics. <http://proceedings.spiedigitallibrary.org/pdfaccess.ashx?url=/data/conferences/spiep/69394/853307.pdf>
1033

1034 Kerr, Y.H., Waldteufel, P., Wigneron, J.-P., Delwart, S., Cabot, F., Boutin, J.,
1035 Escorihuela, M.-J., Font, J., Reul, N., Gruhier, C., Juglea, S.E., Drinkwa-
1036 ter, M.R., Hahne, A., Martin-Neira, M., Mecklenburg, S., (2010) The SMOS

1037 Mission: New Tool for Monitoring Key Elements of the Global Water Cycle,
1038 *Proceedings of the IEEE*, 98(5), 666-687. doi:10.1109/JPROC.2010.2043032

1039 Kerr, Y.H., Waldteufel, P., Richaume, P., Wigneron, J.P., Ferrazzoli, P.,
1040 Mahmoodi, A., Al Bitar, A., Cabot, F., Gruhier, C., Juglea, S.E. and
1041 Leroux, D., (2012). The SMOS soil moisture retrieval algorithm. *IEEE*
1042 *Transactions on Geoscience and Remote Sensing*, 50(5), pp.1384-1403.
1043 doi:10.1109/TGRS.2012.2184548

1044 Kolassa, J., (2013). Soil moisture retrieval from multi-instrument satellite ob-
1045 servations. *Doctoral dissertation, Université Pierre et Marie Curie (Paris*
1046 *6)*.<http://www.theses.fr/2013PA066392>

1047 Kolassa, J., Aires, F., Polcher, J., Prigent, C., Jimenez, C., and Pereira, J. M.
1048 (2013). Soil moisture retrieval from multi-instrument observations: Informa-
1049 tion content analysis and retrieval methodology. *J. Geophys. Res*, 118(10),
1050 4847-4859. doi: 10.1029/2012JD018150

1051 Kolassa, J., Gentine, P., Prigent, C., and Aires, F. (2016). Soil moisture
1052 retrieval from AMSR-E and ASCAT microwave observation synergy. Part
1053 1: Satellite data analysis. *Remote Sensing of Environment*, 173, 1-14.
1054 doi:10.1016/j.rse.2015.11.011

1055 Koster, R.D., Suarez, M.J., Ducharne, A., Stieglitz, M. and Kumar, P., (2000).
1056 A catchmentbased approach to modeling land surface processes in a general
1057 circulation model: 1. Model structure. *Journal of Geophysical Research: At-*
1058 *mospheres*, 105(D20), pp.24809-24822. doi:10.1029/2000JD900327

1059 Lahoz, W.A. and De Lannoy, G.J., (2014). Closing the gaps in our knowledge of
1060 the hydrological cycle over land: conceptual problems. *Surveys in Geophysics*,
1061 35(3), pp.623-660. doi:10.1007/s10712-013-9221-7

1062 Larson, K.M., Small, E.E., Gutmann, E.D., Bilich, A.L., Braun, J.J.
1063 and Zavorotny, V.U., (2008). Use of GPS receivers as a soil moisture
1064 network for water cycle studies. *Geophysical Research Letters*, 35(24).
1065 doi:10.1029/2008GL036013

1066 Leavesley, G.H., David, O., Garen, D.C., Lea, J., Marron, J.K., Pagano, T.C.,
1067 Perkins, T.R. and Strobel, M.L., (2008), December. A modeling framework for
1068 improved agricultural water supply forecasting. *AGU Fall Meeting Abstracts*.

1069 Levenberg, K., (1944). A method for the solution of certain non-linear problems
1070 in least squares. *Quarterly of applied mathematics*, 2(2), pp.164-168.

1071 Liu, Q., Reichle, R.H., Bindlish, R., Cosh, M.H., Crow, W.T., de Jeu, R.,
1072 De Lannoy, G.J., Huffman, G.J. and Jackson, T.J., 2011. The contributions
1073 of precipitation and soil moisture observations to the skill of soil moisture
1074 estimates in a land data assimilation system. *Journal of Hydrometeorology*,
1075 12(5), pp.750-765. doi: 10.1175/JHM-D-10-05000.1

1076 Lucchesi, R., (2013) File Specification for GEOS-5 FP. *NASA Global Modeling
1077 and Assimilation Office (GMAO) Office Note* No. 4 (Version 1.0), 63 pp,
1078 available from http://gmao.gsfc.nasa.gov/pubs/office_notes.

1079 Maeda, T. and Taniguchi, Y., (2013). Descriptions of GCOM-W1 AMSR2 Level

1080 1R and Level 2 Algorithms. *Japan Aerospace Exploration Agency Earth Ob-*
1081 *servation Research Center: Ibaraki, Japan.* suzaku.eorc.jaxa.jp/GCOM_W/
1082 data/doc/NDX-120015A.pdf

1083 Marquardt, D. W. (1963). An algorithm for least-squares estimation of nonlinear
1084 parameters. *Journal of the Society for Industrial and Applied Mathematics,*
1085 *11(2)*, 431-441. doi:10.1137/0111030

1086 McColl, K.A., Vogelzang, J., Konings, A.G., Entekhabi, D., Piles, M. and Stoffe-
1087 len, A., (2014). Extended triple collocation: Estimating errors and correlation
1088 coefficients with respect to an unknown target. *Geophysical Research Letters,*
1089 *41(17)*, pp.6229-6236. doi:10.1002/2014GL061322

1090 McDowell, N. G. (2011). Mechanisms linking drought, hydraulics, carbon
1091 metabolism, and vegetation mortality. *Plant physiology, 155(3)*, 1051-1059.
1092 doi:10.1104/pp.110.170704

1093 Moghaddam, M., Silva, A.R., Clewley, D., Akbar, R., Hussaini, S.A.,
1094 Whitcomb, J., Devarakonda, R., Shrestha, R., Cook, R.B., Prakash, G.
1095 and Vannan, S.S., (2016). Soil Moisture Profiles and Temperature Data
1096 from SoilSCAPE Sites, USA. *ORNL DAAC*, Oak Ridge, Tennessee, USA.
1097 doi:10.3334/ORNLDAAC/1339

1098 O'Neill, P., Chan, S., Njoku, E., Jackson, T., and Bindlish, R. (2015)
1099 SMAP Algorithm Theoretical Basis Document: L2 & L3 Radiometer Soil
1100 Moisture (Passive) Products. *SMAP Project, JPL D-66480*, Jet Propulsion

1101 Laboratory, Pasadena, CA. [https://nsidc.org/sites/nsidc.org/files/](https://nsidc.org/sites/nsidc.org/files/technical-references/L2_SM_P_ATBD_v7_Sep2015-po-en.pdf)
1102 [technical-references/L2_SM_P_ATBD_v7_Sep2015-po-en.pdf](https://nsidc.org/sites/nsidc.org/files/technical-references/L2_SM_P_ATBD_v7_Sep2015-po-en.pdf)

1103 O'Neill, P. E., S. Chan, E. G. Njoku, T. Jackson, and R. Bindlish. 2016. SMAP
1104 L2 Radiometer Half-Orbit 36 km EASE-Grid Soil Moisture, Version 3. Boul-
1105 der, Colorado USA. *National Snow and Ice Data Center Distributed Active*
1106 *Archive Center*. doi:10.5067/PLRS64IU03IT. Accessed: June 2016.

1107 Owe, M., R. deJeu, and J. Walker(2001), A Methodology for Surface Soil Mois-
1108 ture and Vegetation optical Depth Retrieval Using The Microwave Polariza-
1109 tion Difference Index, *IEEE Transactions on Geoscience and Remote Sensing*,
1110 *39*, 1643–1654. doi: 10.1109/36.942542

1111 Philip, J. R. (1957). The theory of infiltration: 5. The influence of the initial
1112 moisture content. *Soil Science*, *84(4)*, 329-340.

1113 Reichle, R. H., and R. D. Koster (2004), Bias reduction in short records
1114 of satellite soil moisture, *Geophysical Research Letters*, *31*,L19501. doi:
1115 10.1029/2004GL020938

1116 Reichle, R.H., Koster, R.D., De Lannoy, G.J., Forman, B.A., Liu, Q., Ma-
1117 hanama, S.P. and Touré, A., 2011. Assessment and enhancement of MERRA
1118 land surface hydrology estimates. *Journal of Climate*, *24(24)*, pp.6322-6338.
1119 doi: 10.1175/JCLI-D-10-05033.1

1120 Reichle, R. H., and Q. Liu, (2014). Observation-Corrected Precipitation Esti-
1121 mates in GEOS-5. NASA/TM 2014-104606, Vol. 35. doi: 20150000725

1122 Reichle, R.H., De Lannoy, G.J., Liu, Q., Colliander, A., Conaty, A., Jack-
1123 son, T., Kimball, J. and Koster, R.D., (2015b). Soil Moisture Active Pas-
1124 sive (SMAP) Project Assessment Report for the Beta-Release L4_SM Data
1125 Product. *NASA Technical Report Series on Global Modeling and Data As-*
1126 *similation*, NASA/TM-2015, 104606, pp.40-63. [https://nsidc.org/sites/
1127 nsidc.org/files/technical-references/Reichle788.pdf](https://nsidc.org/sites/nsidc.org/files/technical-references/Reichle788.pdf)

1128 Reichle, R. H., G. J. M. De Lannoy, Q. Liu, A. Colliander, A. Conaty, T.
1129 Jackson, J. Kimball, and R. D. Koster (2015), Soil Moisture Active Passive
1130 (SMAP) Project Assessment Report for the Beta-Release L4_SM Data Prod-
1131 uct, *NASA Technical Report Series on Global Modeling and Data Assim-*
1132 *ilation*, *NASA/TM-2015-104606*, Vol. 40, National Aeronautics and Space
1133 Administration, Goddard Space Flight Center, Greenbelt, Maryland, USA,
1134 63pp. Available at: <https://gmao.gsfc.nasa.gov/pubs/>

1135 Reichle, R.H., De Lannoy, G.J., Liu, Q., Ardizzone, J.V., Chen, F., Colliander,
1136 A., Conaty, A., Crow, W., Jackson, T., Kimball, J. and Koster, R.D., (2016).
1137 Soil Moisture Active Passive Mission L4_SM Data Product Assessment (Ver-
1138 sion 2 Validated Release). *NASA Global Modelling and Assimilation Office*
1139 *(GMAO) Office Note* No. 12 [https://nsidc.org/sites/nsidc.org/files/
1140 technical-references/Reichle851.pdf](https://nsidc.org/sites/nsidc.org/files/technical-references/Reichle851.pdf)

1141 Reichle, R.H., Liu, Q., Koster, R.D., Draper, C.S., Mahanama, S.P. and Par-
1142 tyka, G.S., (2017). Land surface precipitation in MERRA-2. *Journal of Cli-*
1143 *mate*, 30, pp. 1643-1664. doi:10.1175/JCLI-D-16-0570.1

1144 Reichle, R.H., De Lannoy, G.J., Liu, Q., Ardizzone, J.V., Colliander, A., Conaty,
1145 A., Crow, W., Jackson, T.J., Jones, L.A., Kimball, J.S. and Koster, R.D.,
1146 (2017). Assessment of the SMAP Level-4 Surface and Root-Zone Soil Moisture
1147 Product Using In Situ Measurements. *Journal of Hydrometeorology (in press)*
1148 , doi:10.1175/JHM-D-17-0063.1.

1149 Reynolds, C.A., Jackson, T.J. and Rawls, W.J., (2000). Estimating soil
1150 water-holding capacities by linking the Food and Agriculture Organiza-
1151 tion soil map of the world with global pedon databases and continuous
1152 pedotransfer functions. *Water Resources Research*, 36(12), pp.3653-3662.
1153 doi:10.1029/2000WR900130

1154 Rodrguez-Fernández, N.J., Aires, F., Richaume, P., Kerr, Y.H., Prigent,
1155 C., Kolassa, J., Cabot, F., Jimnez, C., Mahmoodi, A. and Drusch, M.,
1156 (2015). Soil moisture retrieval using neural networks: Application to SMOS.
1157 *IEEE Transactions on Geoscience and Remote Sensing*, 53(11), pp.5991-6007.
1158 doi:10.1109/TGRS.2015.2430845

1159 Rumelhart, D.E., and Chauvin, Y. (1995), Backpropagation: theory, architec-
1160 tures, and applications, *Lawrence Erlbaum Associates*. ISBN: 0-8058-1258-X

1161 Sanchez, N., Martínez-Fernández, J., Scaini, A. and Perez-Gutierrez, C., (2012).
1162 Validation of the SMOS L2 soil moisture data in the REMEDHUS net-
1163 work (Spain). *IEEE Transactions on Geoscience and Remote Sensing*, 50(5),
1164 pp.1602-1611. doi:10.1109/TGRS.2012.2186971

1165 Santi, E., Paloscia, S., Pettinato, S. and Fontanelli, G., (2016). Application

1166 of artificial neural networks for the soil moisture retrieval from active and
1167 passive microwave spaceborne sensors. *International Journal of Applied Earth*
1168 *Observation and Geoinformation*, 48, pp.61-73. doi:10.1016/j.jag.2015.08.002

1169 Schaefer, G.L., Cosh, M.H. and Jackson, T.J., (2007). The USDA natu-
1170 ral resources conservation service soil climate analysis network (SCAN).
1171 *Journal of Atmospheric and Oceanic Technology*, 24(12), pp.2073-2077.
1172 doi:10.1175/2007JTECHA930.1

1173 Schmugge, T.J., Jackson, T.J. and McKim, H.L., (1980). Survey of methods for
1174 soil moisture determination. *Water Resources Research*, 16(6), pp.961-979.

1175 Scipal, K., Holmes, T., De Jeu, R., Naeimi, V. and Wagner, W., (2008).
1176 A possible solution for the problem of estimating the error structure
1177 of global soil moisture data sets. *Geophysical Research Letters*, 35(24).
1178 doi:10.1029/2008GL035599

1179 Seneviratne, S. I., Lüthi, D., Litschi, M., and Schär, C. (2006). Land-
1180 atmosphere coupling and climate change in Europe. *Nature*, 443(7108), 205-
1181 209.doi:10.1038/nature05095

1182 Sevanto, S., McDowell, N. G., Dickman, L. T., Pangle, R., and Pockman, W. T.
1183 (2014). How do trees die? A test of the hydraulic failure and carbon starvation
1184 hypotheses. *Plant, cell & environment*, 37(1), 153-161. doi:10.1111/pce.12141

1185 Stoffelen, A., (1998). Toward the true near-surface wind speed: Error model-
1186 ing and calibration using triple collocation. *Journal of Geophysical Research*,
1187 103(C4), pp.7755-7766. doi:10.1029/97JC03180

- 1188 Su, C.H., Ryu, D., Crow, W.T. and Western, A.W., (2014). Beyond triple
1189 collocation: Applications to soil moisture monitoring. *Journal of Geophysical*
1190 *Research: Atmospheres*, 119(11), pp.6419-6439. doi:10.1002/2013JD021043
- 1191 Tagesson, T., Fensholt, R., Guiro, I., Rasmussen, M.O., Huber, S., Mbow,
1192 C., Garcia, M., Horion, S., Sandholt, I., Holm?Rasmussen, B. and Göttsche,
1193 F.M., (2015). Ecosystem properties of semiarid savanna grassland in West
1194 Africa and its relationship with environmental variability. *Global change bi-*
1195 *ology*, 21(1), pp.250-264. doi:10.1111/gcb.12734
- 1196 Taylor, J.R., Osenga, E.C., Jack-Scott, E., Arnott, J.C. and Katzenberger, J.,
1197 (2015), December. Establishing a Long Term High-Altitude Soil Moisture
1198 Monitoring Network at the Watershed Scale. *AGU Fall Meeting Abstracts*.
- 1199 Wagner, W., Lemoine, G., and Rott, H. (1999). A method for estimating soil
1200 moisture from ERS scatterometer and soil data. *Remote Sensing of Environ-*
1201 *ment*, 70(2), 191-207. doi:10.1016/S0034-4257(99)00036-X
- 1202 Wagner, W., Hahn, S., Kidd, R., Melzer, T., Bartalis, Z., Hasenauer, S., ...
1203 and Rubel, F. (2013). The ASCAT soil moisture product: A review of its
1204 specifications, validation results, and emerging applications. *Meteorologische*
1205 *Zeitschrift*, 22(1), 5-33. doi: 10.1127/0941-2948/2013/0399
- 1206 Walker, J.P. and Houser, P.R., (2001). A methodology for initializing soil mois-
1207 ture in a global climate model: Assimilation of near-surface soil moisture
1208 observations. *Journal of Geophysical Research*, 106(D11), pp.11761-11774.
1209 doi:10.1029/2001JD900149

1210 Wigneron, J.P., Chanzy, A., Calvet, J.C. and Bruguier, N., (1995). A sim-
1211 ple algorithm to retrieve soil moisture and vegetation biomass using passive
1212 microwave measurements over crop fields. *Remote Sensing of Environment*,
1213 51(3), pp.331-341. doi:10.1016/0034-4257(94)00081-W

1214 Zreda, M., Desilets, D., Ferrè, T.P.A. and Scott, R.L., (2008). Measuring soil
1215 moisture content non-invasively at intermediate spatial scale using cosmic-ray
1216 neutrons. *Geophysical Research Letters*, 35(21). doi:10.1029/2008GL035655